Cleaner Materials 19 (2026) 100373

Contents lists available at ScienceDirect

Cleaner Materials

journal homepage: www.journals.elsevier.com/cleaner-materials

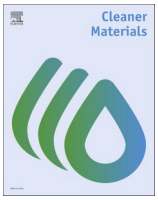

Multifunctional performance assessment of insulation panels from recycled textiles and Kenaf/Hemp Fibers: thermal, acoustic, and fire behavior

Jan Kašpar [a], Giada Kyaw Oo D'Amore [a,b], Jessica Ferrari [c], Enrico Armelloni [c], Vincenzo Ballerini [d], Paolo Valdiserri [d], Eugenia Rossi di Schio [d], Mariagrazia Pilotelli [e], Hossein Soltanian [e], Manuela Neri [e,*]

[a] University of Trieste, Department of Chemical and Pharmaceutical Sciences, Via Valerio 1, 34127, Italy
[b] Department of Engineering and Architecture, Via Valerio 6, Trieste, Italy
[c] University of Parma, Department of Industrial Systems and Technologies, Parma, Italy
[d] University of Bologna, Alma Mater Studiorum, Department of Industrial Engineering, Bologna, Italy
[e] University of Brescia, Department of Mechanical and Industrial Engineering, via Branze 38, Brescia, Italy

ARTICLE INFO

Keywords:
Sustainable materials
Recycled textiles
Natural fibers
Fire resistance
Acoustic properties

ABSTRACT

Although natural and recycled fibre-based insulation materials show promising thermal and acoustic performance, several challenges still limit their widespread adoption. This paper explores the properties and potential of recycled textile and natural fiber-based materials in enhancing building renovations. Specifically, it examines two types of insulation panels: those made from recycled textiles (Panels M) and those composed of kenaf and hemp fibers (Panels K). The study investigates various properties, including composition, density, thermal conductivity, acoustic performance, and fire response, highlighting the strengths and challenges associated with each material. The results reveal that while textile-based panels exhibit more variability in composition and performance, natural fiber panels are more uniform, making them a more predictable and reliable option. Thermal conductivity values ranged from 0.035 to 0.049 W/(m·K), with the natural fiber panels showing more consistent results. Acoustic performance, evaluated using both Sonocat sensor and the impedance tube also varied, with textile-based panel M45 performing particularly well approaching the Basotect performance (this latter used as a functional benchmark). Fire response, tested using Temperature Programmed Oxidation (TPO), indicated that kenaf-based panels demonstrated higher flammability compared to their textile counterparts. Furthermore, the study explored the effectiveness of fire retardants, finding that certain treatments helped suppress ignition.

Introduction

The topic of energy renovation in buildings is complex, involving multiple aspects such as energy poverty, accessibility to available technologies, and materials sustainability. In Europe, approximately 85 % of the building stock was constructed before 2000, with 75 % of it exhibiting poor energy performance (Performance, 2025). This makes the building sector account for half of the total energy consumption, half of all extracted materials, and a third of water consumption (ECORYS, 2025). Given the critical importance of retrofitting buildings to achieve energy independence, Europe has set ambitious goals to accelerate the renovation process, aiming to renovate 35 million buildings by 2030 (Wave, 2025) and to fully decarbonize its building stock by 2050 (Performance, 2025). This is expected to have a substantial impact on reducing energy poverty, defined as the inability to maintain an adequate indoor temperature during both summer and winter. Energy poverty is a growing phenomenon, affecting 6.9 % of citizens in 2021, 9.3 % in 2022, and 10.6 % in 2023 (Energy poverty, 2025).

Despite the availability of various incentives, the building renovation process remains slow and complex, mainly due to multiple barriers. In disadvantaged contexts, the materials and technologies currently available are often unaffordable or require specialized labour for installation, which significantly increases the overall cost of interventions, and price remains the most critical factor in driving or hindering renovation decisions. Noise, dust, and general disruption caused by renovation works frequently discourage homeowners from

* Corresponding author.
E-mail address: manuela.neri@unibs.it (M. Neri).

https://doi.org/10.1016/j.clema.2026.100373
Received 15 April 2025; Received in revised form 31 December 2025; Accepted 1 January 2026
Available online 2 January 2026

pursuing upgrades, and, in multi-owner buildings, obtaining unanimous approval for renovation projects presents a challenge. Additionally, interventions may necessitate permits from local authorities, which lengthens the process and further discourages action. To streamline the renovation process, it is essential to propose solutions that are not only cost-effective and technically feasible but also minimally disruptive. These solutions should be straightforward to implement in individual housing units and manageable by non-specialized workers. However, the choice of insulation materials is essential even in newly built constructions; even if these projects are often targeted at individuals with higher purchasing power, who tend to opt for high-performance – yet more expensive – solutions.

While the goal is to identify cost-effective insulating materials, products intended for the building sector must still meet several essential requirements, including mechanical strength, fire safety, hygiene, environmental protection, accessibility, sound insulation, energy efficiency, and the sustainable use of natural resources (Regulation (EU) No 305/, 2011). Regarding sustainability, in alignment with the European Green Deal (Wave, 2025), there is an increasing commitment across Europe to adopt a circular economy model, which emphasizes the use of sustainable, resource-efficient materials. Indeed, traditional insulating materials, while offering good thermal performance and long-term durability, involve high energy costs for production, disposal challenges, and a significant environmental impact due to the use of fossil-based raw materials. In this context, the use of biomass as a sustainable alternative is particularly promising, thanks to its renewable nature, local availability (depending on the geographical area), and its ability to store CO_2 throughout its life cycle. However, the adoption of biomass-based insulating materials also presents certain challenges, such as the intrinsic variability of their physical and mechanical properties, susceptibility to moisture, and lower consistency and controllability of raw materials compared to conventional industrial products. Despite these limitations, the use of biomass can significantly contribute to reducing the ecological footprint of the construction sector. Additionally, it can have positive economic impacts at the local level, by stimulating employment in the agricultural and bio-construction sectors, and by making certain technical solutions more accessible due to their potentially lower costs compared to synthetic materials. Natural and recycled insulators may not be universally applicable to all building types. However, starting from the needs of vulnerable or underserved segments of the population can foster the development of low-cost, resource-efficient alternatives. Once adequately tested and validated, such solutions can be adapted to a wider range of construction scenarios, including new buildings.

A promising alternative is represented by insulation materials based on natural or recycled fibres. Natural fibres are usually agricultural residues and offer low-cost resources which can support rural economies and promote short supply chains. Numerous studies have explored their potential in the building sector covering a wide range of species, such as coconut, corn, rice, and jute fibres (Abu-Jdayil et al., 2019; Ricciardi et al., 2020; Asdrubali et al., 2015), palm fibers (Benmansour et al., 2014), rice husks (Marín-Calvo et al., 2023), and hemp-based panels (Martínez et al., 2024), as well as the use of these materials as additives in cementitious composites. Animal-based fibres, such as sheep's wool combined with by-products from the textile and agri-industrial local sectors, have also attracted significant interest, such as the combination rice straw, corn residues, textile dust in the Piedmont region (Savio et al., 2022) and hemp, jute from Sardinia (Majumder et al., 2021). Among bio-based materials, wood and its derivatives have garnered growing interest due to their inherent thermal properties, as well as their broad availability (O'Brien et al., 2025). In Thailand, innovative structural sandwich panels have been developed for energy-efficient wall systems, using a laminated oil palm wood core combined with rubberwood-based oriented strand board (OSB) or plywood faces (Jantawee et al., 2023). Reference (Mohammadabadi et al., 2021) reports that full-scale wood composite sandwich panels with cavities filled with closed-cell foam required 74 % fewer strands and, consequently, less resin than standard OSB panels. Wood is used not only as an insulating component in building systems but also as an additive in concrete to improve specific properties. For instance, in (Assal et al., 2025), wood was incorporated into concrete façade elements to investigate the composite's response to thermal variations. In a hotel project in Brazil, traditional hollow block walls were replaced with innovative elements made from Engineered Wood Products (EWP), leading to enhanced sound insulation—both between rooms and at the façade—and an increase in thermal resistance from 0.50 to 1.86 m^2K/W (Ribeiro et al., 2025). It is worth noting, however, that the sustainability of such fibres may be affected using chemical treatments required to improve resistance to fire, mould, and pests (Berardi and Iannace, 2015). In (Halashi et al., 2024), loofah panels with a bio-based binder exhibited a Sound Absorption Average (SAA) values between 0.16 and 0.68 and Keff between 0.033–0.054 W/(m·K). Greater thickness and optimized density ensured the best performance, while binder content had no significant effect. Optimal conditions (40 mm, 225 kg/m^3, 7.5 % binder) yielded superior acoustic and thermal properties, validated by simulations and predictive models.

The textile sector, which is one of the most resource-intensive industries, also plays a role in promoting sustainability. The EU Strategy for Sustainable and Circular Textiles (Press-release, 2023) encourages the reuse and recycling of textile materials. With approximately 12 kg of textile waste per person annually, less than 1 % of textiles are recycled globally (Press room, 2025). One of the main challenges in textile recycling is meeting quality standards: limitations in mechanical sorting processes, lead to a reliance on incineration and landfilling as predominant waste treatment methods (Tanguay-Rioux et al., 2021; Solis et al., 2024). Textiles have been converted into insulation materials, with various types of fibres such as carpet waste (Rushforth et al., 2007), crushed carpet edges (Miraftab and Goswami, 2018), upholstery fabrics (Hadded et al., 2016), and linter (Tallini and Cedola, 2018) being utilized. The study in (Hassani et al., 2024) shows that fibre panels from recycled denim provide good sound absorption and fire resistance, offering a sustainable solution for construction and automotive applications. Performance depends on thickness and density: higher values enhance acoustic absorption, while increased density and binder content reduce flame spread. Under optimal conditions (0.027 m thickness, 140 kg/m^3 density, 43 % binder), SAA reached 0.538 and the Flame Advancement (FA) 53.1 mm/min.

Within the framework of circular economy and with the aim of proposing materials accessible to all, recent studies have investigated the thermal properties, fire resistance, and acoustic behavior of waste materials from the production of surgical masks as well as of the masks themselves (Neri et al., 2023; Al et al., 2024; Di Schio et al., 2024; Dehdashti et al., 2024). The study proposed in (Neri et al., 2023), analyzed recycled polyamide-66 fiber and it demonstrated better thermal performance than commercially-available recycled cotton insulation, achieving similar thermal resistance values with lower insulation bulk densities. The study reported in (Al et al., 2024) analyzed composite materials developed by incorporating date palm leaves (used as filler) into polypropylene from recycled face masks. The composites demonstrated thermal conductivity values as low as 0.069 W/(m·K), acoustic absorption coefficient of 0.4. Thermogravimetric analysis showed a high thermal stability for the composites, with degradation temperature exceeding 300 °C. The study in (Di Schio et al., 2024) focused on the properties of surgical face masks in different configurations, and it was found that water vapor permeability is comparable to mineral and glass wool, with thermal conductivity ranging from 0.039 to 0.072 W/(m·K), typical of fibrous materials. Conductivity depended on arrangement, density, while sanitization and flame-retardant treatments increased conductivity without a clear trend. The fire behaviour analysis showed that fire protection requires embedding panels in gypsum boards. However, in (Dehdashti et al., 2024) the addition of a bio-based binder was investigated, and panels with different thicknesses,

densities, and spunbond-to-meltblown blending ratios were analyzed. Their fire performance was also tested, with all panels exhibiting self-extinguishing properties.

Textile fibres have additionally been incorporated as additives to enhance the properties of cementitious materials. For example, the study in (Sadrolodabaee et al., 2025) developed a sustainable material for paving flags by reducing Portland cement content, incorporating waste textile fibers, and replacing natural aggregates with recycled construction waste. The aim was to enhance decarbonization potential while maintaining technical performance. Results demonstrated adequate mechanical strengths, strain-hardening behavior, durability against freeze-thaw and abrasion, confirming both technical and environmental feasibility. In (Sadrolodabaee et al., 2022), fibre cement boards reinforced with natural and recycled synthetic textile fibers were developed to improve technical performance and reduce environmental impact. Tests showed good fire resistance and effective thermal and acoustic insulation. Sustainability was assessed through a model integrating economic, environmental, and social indicators, yielding an index between 0.68 and 0.71, confirming the material's technical and environmental feasibility.

Although these materials show promising thermal and acoustic performance, several challenges still limit their widespread adoption. Key issues include fire behaviour, property homogeneity – particularly difficult to achieve with recycled fibers due to sorting limitations – and long-term durability. For instance, the influence of the production method and surface treatment on the thermophysical characteristics and behavior under direct fire of two polyethylene terephthalate non-woven fabrics was investigated in (Petkova-Slipets et al., 2022). It was found that non-woven polyester with acrylic additives and adhesive bonding has a higher thermal conductivity value and high flammability with complete combustion. In contrast, thermosetting siliconized polyester materials have limited flammability with limited droplet release. The silicone-based finish protects the polyester fibers leading to self-extinguishing and stopping the complete combustion of the sample.

Additionally, the lack of standardized procedures for testing and certifying these materials results in high costs for obtaining CE marketing, requiring a European Technical Assessment (ETA) (European Organisation for Technical Assessment, 2025). For insulation products based on plant or animal fibres, assessment frameworks such as EAD 040005-00-120 (EAD 040005-00-1201), and for polyester fibers such as the EAD 040288-00-1201 (EAD 040288-00-, 2025) specify the required tests – ranging from thermal conductivity and reaction to fire to moisture resistance and biological durability. These technical and regulatory hurdles contribute to the continued dominance of traditional insulation materials, such as mineral wool and glass wool, in the construction market.

The aim of this article is to evaluate selected properties of materials based on natural fibers and on recycled textile fibres respectively, to understand their potential positioning in the market compared to other commercial materials. Specifically, as shown in Fig. 1, the materials analyzed are panels K made of kenaf and hemp fibers, and panels M made of recycled textile. The panels are produced by a manufacturer specialized in the production of insulating materials for the building sector made of natural and recycled fibers, such as kenaf, textile, wood fibers, recycled paper, and polyester. Today, the company is focusing decisively on textiles, thanks to the high availability of raw materials from, textile production, technical clothing and the entire high quality manufacturing chain.

The study presents a multidisciplinary approach, focusing on specific aspects. Rather than replicating standardised testing procedures – as the materials analysed have already been tested in certified laboratories – alternative techniques have been employed, to investigate

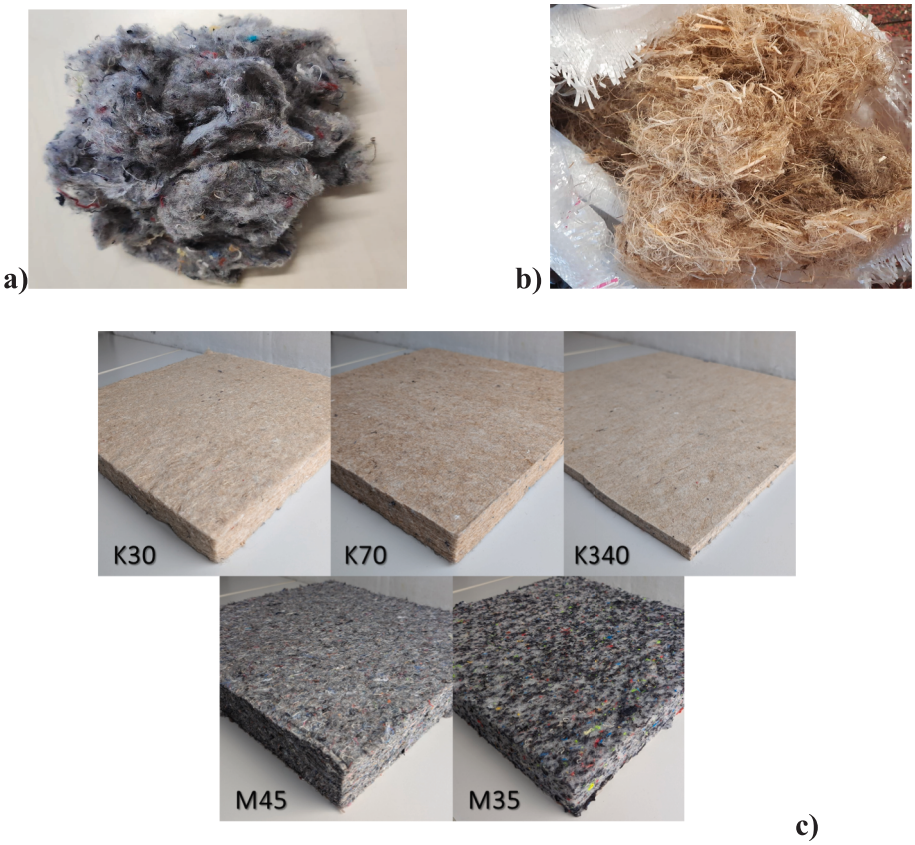

Fig. 1. Materials analyzed in this study: **(a)** recycled textile fibers used to produce M−type panels; **(b)** a mix of kenaf and hemp fibers used for the fabrication of K-type panels. These raw materials are processed by the manufacturer to obtain the final insulation panels **(c)**. Specimens analyzed: K30, K70, and K340 panels are composed of kenaf and hemp fibers, while M45 and M35 panels are made of recycled textile fibers. All panels contain polyester as a binding agent.

characteristics that would otherwise remain undetected. The analysis focuses on the panels composition and density, which can vary significantly depending on the types of fibres used. Therefore, a comparison has been proposed between measured densities and the manufacturer's declared values, and the panel's composition is examined using infrared spectroscopy. Variations in these properties can influence other performance factors, such as thermal conductivity, acoustic performance, and fire resistance. Thermal conductivity is assessed using the heat flow meter method, while acoustic properties (sound absorption and insulation) are measured using the Sonocat multi-array sensor and Kundt's tube. In addition to the materials under investigation, two well-documented materials – Basotect and EPS – are used as reference materials (as functional benchmarks) for sound absorption comparison, since the former represents an excellent sound-absorbing material, while the second one is acoustically reflective. Since they represent the two acoustic extremes – significant absorption and significant reflection – provides a comprehensive comparison framework, allowing the recycled and natural fiber panels to be positioned relative to both materials, thus enabling complete evaluation of their acoustic performance across the absorption spectrum. Fire resistance is assessed using Temperature Programmed Oxidation (TPO), which provides detailed data on ignition temperature, smoke composition, and gas production. Testing was conducted across multiple laboratories, including thermal tests at the University of Bologna, acoustic tests at the University of Parma and University of Trieste, and fire response tests at the latter.

The novelty of this study lies in the adoption of a multidisciplinary and non-conventional approach, integrating alternative analysis techniques (actual vs declared density, IR spectroscopy, Sonocat, TPO) to highlight properties of natural and recycled fiber panels that cannot be detected through standardized tests. It should be noted that the present study has focused exclusively on the thermal, acoustic, and fire performance of the investigated systems. Other aspects relevant to renovation adoption — such as hygrothermal behavior, long-term mechanical stability, mold and VOC risks, as well as life cycle and cost assessments — were not included in the scope of the current tests. These dimensions are regarded as complementary and necessary research directions, which will be addressed in future work to provide a more comprehensive and integrated evaluation of the system's performance and impact.

The structure of the paper is as follows: Section 2 provides an overview of the materials analyzed, Section 3 outlines the theoretical background, research methodology, and laboratory testing procedures, and Section 4 presents the experimental results and their discussion. Then, the Conclusions summarize the key findings and implications for future research.

Materials and methods

The experimental study has been conducted through a comprehensive series of tests, focusing on four main aspects: panel characterization, thermal performance, acoustic behavior, and fire response. Two types of materials have been analyzed; as shown in Fig. 1, panels K are made from kenaf and hemp fibres (Fig. 1 a), while panels M are made of textile fibres (Fig. 1 b); polyester is added as the fibre-binding agent in both panel types. Fig. 1c shows the final products available on the market and considered in the experiments.

The fibers used in the M panels are sourced from clothing manufacturers, either as production waste fabrics or unsold garments, which, due to brand policy, cannot be resold. These garments are collected by specialized companies that remove non-textile components, such as zips and buttons, before shredding the fabric to obtain the fibers shown in Fig. 1 b). According to the manufacturer, no wool is used, but the exact composition percentages of the fibers remain unknown, as each fabric contains various types of fibers. To remedy the lack of this data, a composition analysis was performed through the infrared spectra technique as described below. The manufacturer recommends installing these panels between two layers of bricks to prevent direct flame exposure in the event of a fire, and provides information on certain properties of the products, such as dynamic stiffness and fire reaction classification, based on tests carried out in certified laboratories.

Table 1 summarises the experimental tests performed in this study and the type of panels tested. For textile fibre materials, a single type of panel was analysed, the one that the manufacturer claims has a density of 40 kg/m^3. For kenaf fibre panels, three different densities were chosen, respectively 30, 80 and 480 kg/m^3, again according to the manufacturer. This range made it possible to assess how density influences the production of smoke.

The panel density was determined as a medium value between three samples, which were maintained for a week in a room with controlled ambient conditions. Specifically, the temperature and humidity were 22 °C and 55 % respectively. The panels have been qualitatively characterized using infrared spectroscopy. Thermal performance has been investigated by measuring the thermal conductivity using the heat flow meter technique. Acoustic characteristics have been assessed using two methodologies: the Kundt's tube, designed for small samples, and the Sonocat methodology, which employs an array of microphones for in-situ measurements (Consten et al., 2019). Two additional materials, Basotect and EPS, were used in the acoustic tests as functional benchmarks. While these reference materials differ structurally from the fiber-based panels (foam vs. fibrous structure), they were selected to provide performance benchmarks representing the acoustic extremes typically encountered in building applications: significant sound absorption (Basotect) and good sound reflection (EPS). This comparison framework allows positioning the recycled and natural fiber panels within the existing acoustic performance landscape available to designers and specifiers, focusing on functional equivalence rather than structural similarity.

Results of tests performed by the producer according to the UNI EN 13501–1 (UNI EN, 2018) showed that both the K70 and the M35 panels are classified as flammable, with self-sustained combustion and a tendency to char, which corresponds to a E classification. Such certification, however, does not provide indications on the nature and quantity of the evolved gases, which is seldom addressed in the literature, despite being particularly important: the majority of casualties during fires are due to asphyxiation or poisoning. In this study the materials fire response has been examined by using a Temperature Programmed air-Oxidation (TPO) to detect the ignition temperatures and provide a quantitative and qualitative determination of evolved gases. The panel that showed the greatest criticality in terms of fire behaviour (K30, as described in detail in the following paragraphs) was treated with flame retardant at different concentrations to determine its effects on ignition and gas evolution: the panels thus obtained have been identified with specific acronyms indicating the percentage of treatment applied, K30-FR1.8 % and K30-FR13% (Fig. 2).

FT-IR characterization of the materials

To provide a fingerprint of the materials' chemical composition, the infrared spectra technique was used, by means of the FT-IR spectroscopy using FT-IR Affinity-1S with ATR accessory (manufactured by Shimadzu, Japan). In this study, 20–30 mg of the material under investigation was introduced into the U-shaped microreactor between two layers of quartz, as depicted in Fig. 3. A 30 mL/min gas flow of synthetic air was set through the reactor, using 23.72 mL/min of N_2 and 6.28 mL/min of O_2 to obtain a 20.95 % v/v concentration of O_2. At the outlet of the reactor, a make-up flow of 270 mL/min of N_2 has been added to achieve rapid transfer of the sample into the FT-IR gas cell. Temperature has increased at a uniform rate (Gervasini and Auroux, 2013).

Fire response analysis using temperature Programmed Oxidation (TPO)

The fire performance standard for construction products and components UNI EN 13501–1 (UNI EN, 2018) outlines procedures for testing

Table 1
Samples identification and list of the tests performed on the different panels. The analysis of the panel's characteristics regards the density measurement and the definition of the composition using infrared spectroscopy. The acoustic tests have been performed also on Basotect and EPS for comparison. Fire reaction tests were carried out on both untreated panels and panels treated with flame retardants. The effectiveness of the treatment was analysed on the K30 panel in particular, as it showed the worst performance in terms of fire resistance.

Panel characteristics					**Experimental tests performed**					
					Panel composition	Thermal tests	Acoustic tests		Fire response	
Sample	**Materials**	**Declared density [kg/m^3]**	**Measured density [kg/m^3]**	**Thickness [mm]**	**FT-IR**	**Heat flow meter**	**Kundts tube**	**Sonocat**	**Ignition temperature and gas production**	**Fire retardant effect**
M35	Textile with polyester binder	40	36	50	x	x	x	x	x	
M45		40	45	50	x		x	x	x	
K30	Hemp and kenaf with polyester binder	30	31	40	x	x	x	x	x	x**
K70		80	71	40	x	x	x	x	x	
K340		480*	340*	10			x	x	x	
Basotect		*9*		*50*			x	x		
EPS		*15*		*60*			x	x		

* Measured density values are somewhat different from those declared, particularly in the case of the K340 sample.
** The samples treated with fire retardant are denoted as K30-FR1.8% and K30-FR13% depending on the fire-retardant dilution.

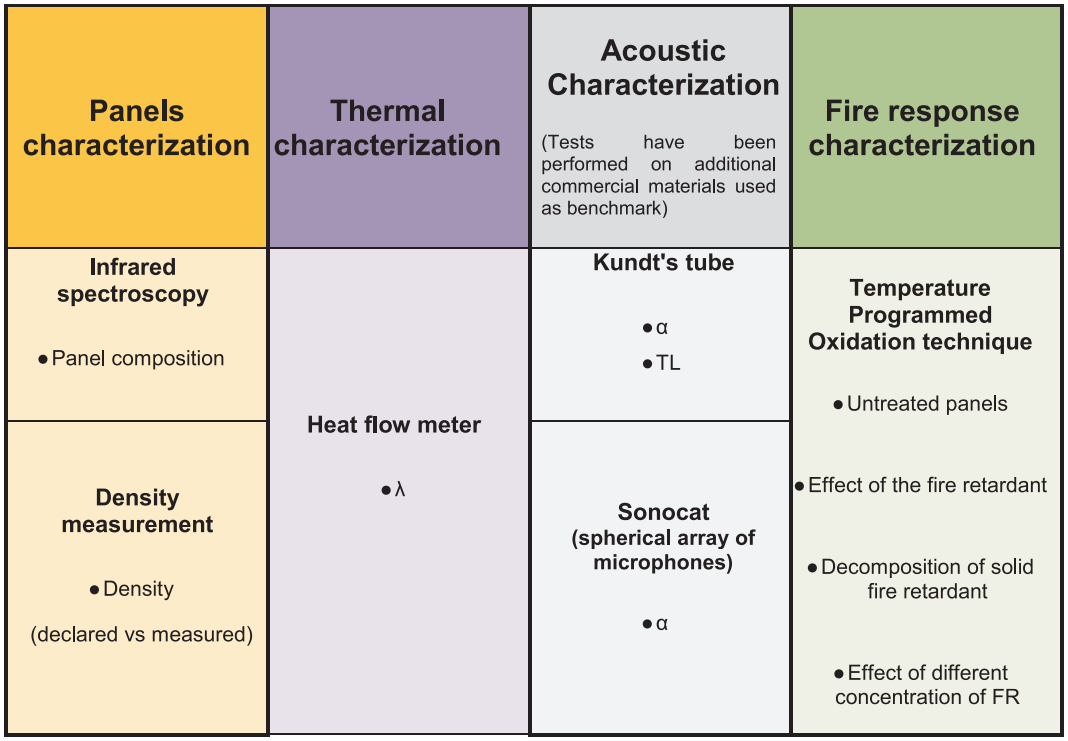

Fig. 2. Schematic representation of the experimental campaign which includes four types of analysis: (1) *panel characterization*, focusing on the composition and density measurement of the panels; (2) *thermal conductivity testing*; (3) *acoustic performance evaluation* using two complementary techniques; and (4) *fire response characterization*, including an investigation into the effect of flame-retardant treatment applied to one of the analysed panels.

materials used in construction. Key tests used to classify the fire performance of construction materials are reported in (International Organization for Standardization ISO, 1182; International Organization for Standardization ISO, 2020; International Organization for Standardization ISO, 1716; UNI EN, 2020; International Organization for Standardization ISO 9239-1:, 2010). The result of these tests is the materials' fire resistance classification, and it encompasses non-combustible materials (classes A2 – A1), non-flammable or difficult-to-flame, combustible materials (classes B and C), normally flammable, combustible materials (classes D to E), and easily flammable combustible materials (classes E and F). The tests evaluate several aspects, but they do not address the qualitative and quantitative analysis of gases produced during the decomposition of the materials. In fire incidents, toxic gas emissions and oxygen depletion are significant contributors to fatalities. Flame retardants can be very useful in reducing smoke production (Green, 1996) and increasing the ignition temperature. Therefore, flame

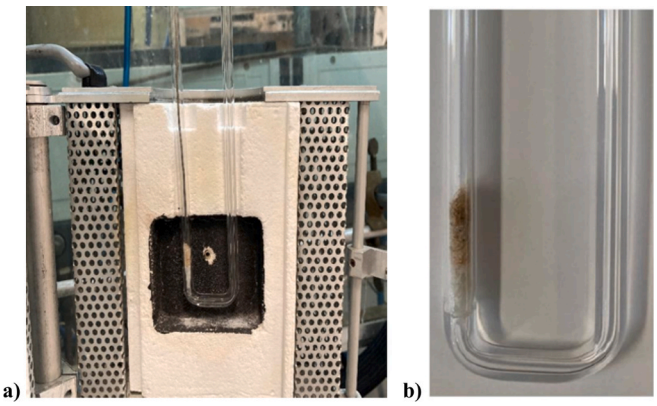

Fig. 3. TPO apparatus: U-tube flow reactor mounted in the electric oven (**a**), and detail of the reactor containing insulation material (**b**).

retardants in building insulation panels are very important; between 60 an d 80 % of fire deaths are caused by smoke inhalation or a combination of burns and inhalation of gases (Lee-Chiong, 1999), and flame retardants can be helpful in preventing these deaths.

The tests presented in this section aim to assess the ignition temperatures of the panels and to detect the quantity and nature of the gases produced. Specifically, the measured gases include carbon dioxide, carbon monoxide, acetaldehyde, formaldehyde, methane, nitrogen monoxide, nitrogen dioxide, water, ammonia, and isocyanic acid. These tests were chosen in place of standard fire resistance tests because, while the latter are mandatory, performed by the producer, to classify materials based on fire resistance, they do not provide information on the qualitative and quantitative aspects of the gases released during combustion. As quoted above, the release of toxic gases and the depletion of oxygen are the leading causes of fatalities in fire incidents. In this study, the TPO technique is not proposed as an alternative certification method; instead, it is proposed to analyze aspects neglected by this regulation, *e.g.* gas evolution in the fire, their nature, amount, and toxicity. Data obtained can easily provide information on how dangerous the material in case of fire is, and that would be an important piece of information for the consumer.

Accordingly, the panels were characterized through the Temperature Programmed Oxidation (TPO), a simple laboratory technique typically employed for solid materials (Jones and McNicol, 1986). It consists of heating a sample in the flow of a gas or a gas mixture. The TPO experimental apparatus is shown in Fig. 3 and comprises a gas line for pretreatments, a U-type reactor inserted in an electrically heated oven, and an FT-IR detector (MKS MultiGas 2030 FT-IR made by MKS Instrument, ESA) for qualitative and quantitative analysis. The MultiGas 2030 instrument measures the roto-vibrational spectra of the gaseous samples. The identification of the nature of the gases is carried out by comparison of the experimental spectra with those of calibration mixtures, whereas quantification is performed using calibration curves that were generated using calibration mixtures. The calibration mixtures were prepared by employing a dilution system equipped with Brooks 5850E series flowmeters to dilute the gas mixture and obtain a low concentration of CO_2. It is important to note that each gas has its own gas factor. In a typical TPO analysis, 20–50 mg of the sample cat-off from the panel were loaded in the reactor and heated (10 °C min^{-1}) up to 550 °C and held at this temperature for 30 min in a flow of synthetic air (30–100 mL^{-1}).

The tests were performed on samples taken from both untreated panels and fire-retardant-treated panels, with qualitative and quantitative analyses conducted to compare gas emissions and assess the effects of the fire retardant. This analysis involved several sub-steps, that is, analysis of the decomposition of the solid FR and the effect of the impregnation of the panel with solutions at different FR concentrations. Since the K30 sample appeared to be the most susceptible to ignition (see Table 2) during thermal treatment, this sample was used in this study. Samples (5 g) were dried at 60 °C for 16–17 h, and then soaked in 100 mL of FR solution, either pure or diluted (1:10 vol), for 5 min. These samples were then thoroughly drained and dried at 60 °C for 6 h and stored in a dryer before use. A 13 w/w% weight gain was observed using pure FR solution, while for the dilute treatment, a 1.8 w/w% weight gain was recorded. The weight gain is associated with the amount of FR deposited. The treated sample will henceforth be referred to as the 'weight gain'. Thus, K30-FR13% represents the K30 sample treated with the pure solution of FR, while K30-FR1.8 % represents the K30 sample treated with the dilute solution of FR.

Thermal conductivity assessment

The panels' thermal conductivity has been measured by means of a homemade heat flow meter designed to analyze materials with thermal conductivities less than 5 W/(m·K), adhering to the ISO 8301 (International Organization for Standardization 8301:, 1991) standard. Samples sized 0.50 x 0.50 m were obtained and, for each analyzed panel, three tests were conducted after a conditioning process to remove residual moisture from the panels until the weight change over 24 h was less than 1 %. The panels were positioned between two plates, one hot and one cold, maintained at different but constant temperatures by conditioned water from two thermostatic baths. When the system was in a quasi-steady state corresponding to a heat flow variation of less than 0.5 %, temperature, and heat flow data were collected, and the thermal conductivity λ was calculated according to the UNI EN 12667 (UNI EN, 2002) standard.

Acoustic characterization

In building acoustics, it is crucial to distinguish between sound insulation, described by the transmission loss (TL), and sound absorption, represented by the sound absorption coefficient (α). Sound insulation refers to a material's ability to block sound transmission between spaces (mostly related to partition walls or facades), while sound absorption represents the capacity to convert sound energy into thermal energy, reducing echoes and reverberation within a space. Notably, a material that insulates well may not necessarily absorb sound effectively, and vice versa, and the choice of materials – whether insulating, absorbing, or a combination – depends on the specific acoustic objectives of the space. Fig. 4 shows the path of a sound wave interacting with a partition.

The sound absorption coefficient α, tells how much of the sound energy hitting a surface is absorbed rather than reflected into the same room. This parameter is fundamental for controlling and reducing reverberation (echo) and noise levels within a single space. The absorption mechanism is based on the conversion of sound energy into a small amount of heat, effectively removing the sound from the environment. For this reason, sound-absorbing materials are often porous and fibrous, such as acoustic foams or mineral wool, which allow sound waves to penetrate the structure and dissipate energy through internal friction. The coefficient α is measured on a scale from 0 to 1, where each value has a precise physical meaning. A value of $\alpha = 0$ indicates a perfect reflector, such as polished marble, which completely reflects the incident sound energy. At the opposite extreme, $\alpha = 1$ represents a perfect absorber, comparable to an open window, since the sound that passes through the opening does not return to the original environment. From an energy perspective, the coefficient is based on the relationship between three fundamental components: the incident sound (W_o), the reflected sound (W_r), and the absorbed sound (W_a). As correctly indicated in the formula, α represents the ratio between the absorbed energy and the incident energy:

$$\alpha = W_a/W_o \quad (1)$$

The TL quantifies the amount of sound energy that is prevented from

Table 2
Quantitative analysis of the gases evolved during the TPO experiments from the samples. Results for panel K30 treated with fire retardant (FR) at different concentrations are also included.

Measured value (unit) (standard deviation)	M35	M45	K30	K70	K340	K30-FR1.8 %	K30-FR13%
V gas/mass (L/g) (0.02)	0.41	0.54	0.60	0.50	0.45	0.53	0.50
V CO_2% (%) (1.3)	64.00	69.79	78.93	68.44	67.68	64.08	75.38
V CO (%) (1.3)	28.09	27.09	18.70	28.62	26.43	33.80	19.98
V Acetaldehyde (%) (0.06)	7.03	1.90	1.04	1.56	4.61	0.92	1.12
V Formaldehyde (%) (0.02)	0.50	0.69	0.35	1.18	1.01	0.33	0.12
V NO (%) (0.02)	0.24	0.44	0.16	0.05	0.04	0.14	–
V CH_4 (%) (0.16)	0.13	0.10	0.82	0.16	0.24	0.23	0.30
V NH_3 (%)	–	–	–	–	–	0.12	1.66
V HNCO (%)	–	–	–	–	–	0.38	1.44
T ignition (° C) (2)[a]	–	–	460	484	474	–	–
T decomposition (° C) (3)[b]	175	231	173	187	203	121	120

[a] Temperature corresponding to the peak in the temperature profile associated with autoignition.
[b] Temperature at which gas evolution starts.

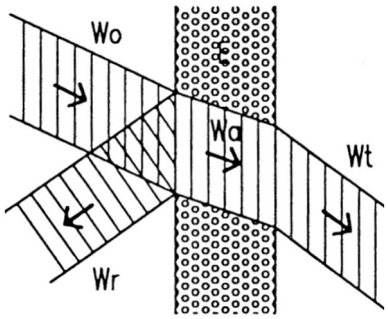

Fig. 4. Decomposition of a sound wave interacting with a partition. W_o represents the incident component, W_r the reflected component, W_a the absorbed component, and W_t the transmitted component.

passing through the material from the source room to the receiving room, with higher TL value indicating less sound power transmitted to the receiving room. In simple terms, α and TL measure two different ways in which a material interacts with sound.

In the acoustic experiments presented in this paper, two techniques have been used: the Kundt's tube – or impedance tube – shown in Fig. 5, and the Sonocat microphone array shown in Fig. 6. The use of both methods allowed to compare a standardized measurement regulated by international norms with a more innovative, non-standardized approach, providing a comprehensive understanding of material acoustic performance, and provides valuable insights into the practical applicability of the tested materials.

The Kundt's tube represents the traditional laboratory method designed to measure α and TL of small samples following established ISO standards. This approach provides standardized, repeatable measurements that are universally recognized and considered reliable within the scientific community. The controlled laboratory environment eliminates external variables, ensuring measurement precision and enabling direct comparison with literature data. To capture material variability, these tests were conducted on samples extracted from various positions across the panels. The detailed derivation of the impedance-tube four-pole method is provided in the Supplementary Information (Eq. S1–S3).

In contrast, the Sonocat microphone array was used for in-situ measurements of α on larger specimens, representing a more innovative and flexible approach that is not yet regulated by international standards. While this method operates in a less controlled environment with all the variables of real-world conditions, it offers the significant advantage of measuring actual material performance as it would behave in practical applications. The Sonocat measurements reveal how materials perform in real-world scenarios where factors such as edge effects, mounting conditions, and environmental variables may influence acoustic behaviour. These tests were performed at different locations on each sample to evaluate the robustness and repeatability of the results under realistic conditions.

Experimental setup

The measurements were conducted on 50 × 50 cm samples, positioned on the laboratory's tiled floor to simulate a reflective plane. To compare the performance of materials made of raw fibres and those of recycled fibres, further tests were performed on commercial insulating panels Basotect and EPS (expanded polystyrene) utilized as functional benchmarks. The first one is a melamine foam, well-documented in the literature, while EPS is a closed-cell structure material.

A compact LG speaker 10 × 10 × 14 cm in dimension was placed at

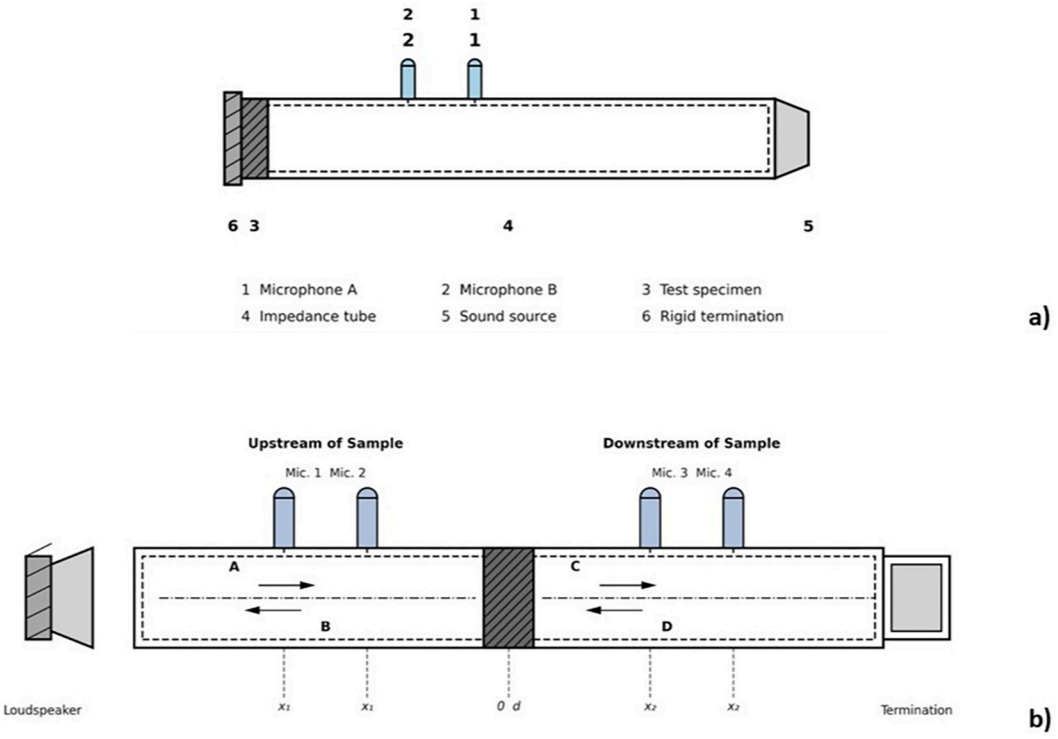

Fig. 5. Kundt's tube setting for the measurement of the sound absorption coefficient **(a)**, and the TL with the two loads technique **(b)**. The configuration in (a) includes two microphones (Mic. A and B), a sound source, and a rigid termination, with the test specimen placed inside the impedance tube. The configuration in (b) features four microphones (Mic. 1–4), a loudspeaker, and defined distances (x_1, x_2, d, and x_3). The test sample is positioned centrally within the tube and backed by a terminating load.

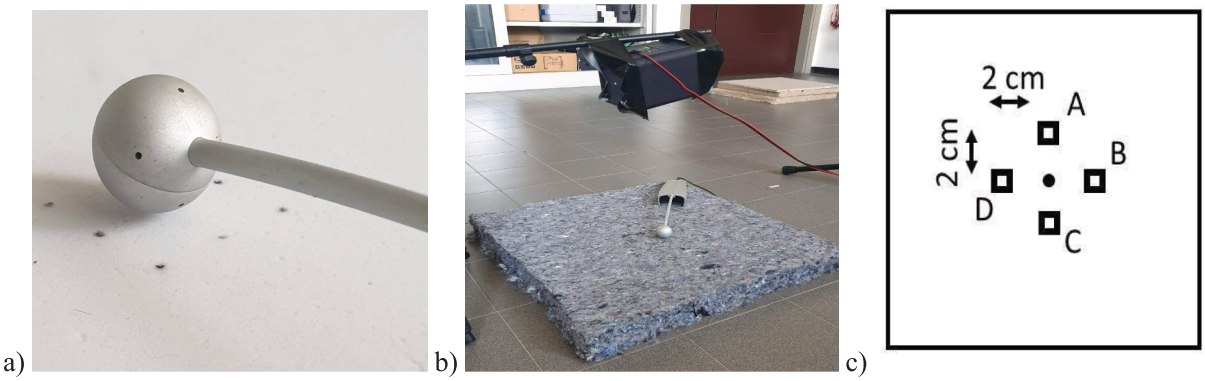

Fig. 6. Experimental setup for the acoustic tests performed with the Sonocat sensor **(a)**. The sensor is equipped with a spherical array of 8 MEMS microphones (30 mm). Positioning of the sensor and the loudspeaker over the panel **(b)**, and scheme of the measurement points **(c)**. The measurements were taken at five points: one at the center of the specimen, and four others positioned 2 cm away from the center along the vertical and horizontal axes.

50 cm from the sample and carefully centred. An exponential sine sweep signal of 10 s was the excitation source, covering the entire audible spectrum from 20 Hz to 20 kHz. The Sonocat instrument was instead positioned at 1 cm from the sample surface. The acquired data were processed by Sonocat's dedicated software, which provides α in third-octave bands for each measurement point, allowing a detailed analysis of the spatial variability of the material's acoustic properties.

To obtain a representative sample characterization, the diamond pattern schematized in Fig. 6 c) was adopted: four measurement points (A, B, C, and D) were arranged equidistant from the centre by 2 cm. At each point, repeated measurements have been taken and their results have been subsequently arithmetically averaged to obtain a more representative and statistically robust value. Noticeably, the Sonocat may report negative α values when the measured reflected power exceeds the incident power; this does not indicate negative energy (which is physically impossible) but rather signals that the material is emitting sound energy instead of absorbing it. The software interprets this situation as an "emission coefficient", displaying it with a negative sign. Accordingly, the negative sign thus serves as a diagnostic indicator for the operator.

For impedance tube measurements, three samples were tested for each panel typology to evaluate material homogeneity, and each sample underwent three repeated measurements to assess repeatability. The curves represent the average of these three repetitions per sample, with a standard deviation of 0.001. For Sonocat measurements, tests were performed at multiple locations on each panel to evaluate spatial variability. Repeatability at the same measurement point showed variations within 3 %, while measurements at different locations demonstrated

contained variability with a maximum deviation of 4 % from the mean value.

Results and discussion

In this Section, the results of the experimental campaign are presented and discussed.

Panels characterization by means of infrared spectroscopy

A perusal of the images of the samples reported in Fig. 1c reveals that there are clear differences among them, particularly between the M35 and M45 ones (the colour of these latter two samples is different), even though they are described by the producer as equivalent ones. Further, the specific composition of insulation materials as deduced from datasheets is often imprecise, and relative percentages of the components are normally never given. To identify the possible impact of sample composition on the investigated properties and to assess the sample consistency in the case of formally equivalent materials, i.e. M35 and M45, the i.r. spectroscopy was employed, which is an easy, rapid, and inexpensive method to compare and identify with reasonable certainty the chemical composition of different materials.

Generally speaking, the infrared spectra provide a fingerprint of the materials' chemical composition at a molecular level; accordingly, the similarity of the spectra patterns indicates equivalent sample composition. The infrared spectra of K30, K70, and K340 materials are reported in Fig. 7. Whereas samples K30 and K70 feature comparable spectra, sample K340 presents, under comparable spectrum acquisition conditions, significantly higher absorbance, yet, with the exclusion of the zone between ca. 900–1150 cm^{-1}, a comparable pattern to the other two samples.

Fig. 8 reports the spectra of the M35 and M45 samples; again, there are clear differences in the two spectra, particularly in the 750–1150 cm^{-1}. The comparison with the spectra reported in Fig. 7 suggests similarities in the spectra of M35 and K340 samples. In the literature, sharp peaks at 1712 cm^{-1}, 1240 cm^{-1}, and 722 cm^{-1} are attributed to the presence of polyesters, which are used as binders.

To discriminate the contribution of the polyester binder, Fig. 9 reports two sets of comparisons of the panel materials with the spectrum of a commercial polyester polymer. All of them have been normalized on the intensity of the peak at 1712 cm^{-1}, which is unequivocally attributed to the carbonyl group of the polyester. The comparison clearly indicates that polyester IR features dominate the spectra of samples M45 and K340, whereas M35 and K70 (K30 is not reported for clarity since its pattern is comparable to K70) features a number of peaks/peak patterns in the ranges 750–1150 cm^{-1} and around 3200 cm^{-1} (OH stretching) not attributable to the polyester (peaks denoted in azure in Fig. 9 b). As a matter of fact, the former bands are attributable to the cellulose, hemicellulose, and lignin constituents of natural fibers. The dominance of polyester in the IR spectrum of the K340 materials appears in line with its high density, which requires higher amounts of the binder compared to the other samples (K30 and K70), which reasonably covers the surface of the fibers, thus accounting for the observation. At lower binder content, kenaf/hemp spectral features are discernible in the less dense materials. Accordingly, the difference in the spectra of M35 and M45 can be attributed to the presence of mostly synthetic-polyester fibres in the former panel, whereas for the M45 panel, evidence is reported that recycled fibres contain a significant number of natural fibres.

Thermal conductivity

The thermal conductivity was measured for M35, K30, and K70 samples. Each measure has been repeated three times, yielding to the value $\lambda = 0.044$ W/(m•K) (with RMSE 0.0014) for M35, $\lambda = 0.049$ W/(m•K) (with RMSE 0.00047) for K30, and $\lambda = 0.035$ W/(m•K) (with RMSE 0.0) for K70, displaying good repeatability especially for the high-density panel. For all the considered samples, indeed, the conductivity values are within the range of interest for possible applications in thermal insulation. The more causal composition of material M yields less homogeneous samples. A comparison of the measures of the kenaf and hemp samples K30 and K70 indicates that the thermal conductivity is a decreasing function of the panel density.

Few scientific papers deal with the measurement of the thermal conductivity for textile materials as a function of the density, emphasizing the discrepancies and inconsistencies (Yang et al., 2020). However, the technical sheets supplied by the manufacturers and engineering manuals (ASHRAE Handbook of Fundamentals, 2017) highlight, for many building' materials, a "U"-shaped behaviour, with a minimum arising for a density value that depends on the material. Indeed, our findings of a thermal conductivity as a decreasing function of the panel's density is perfectly compatible.

Acoustics characterization

In this section, the results of the acoustic tests conducted using the Kundt's tube and the Sonocat sensor are presented and discussed. It is important to note that the samples analyzed with the Kundt's tube are cylinders with a diameter of 4.5 cm, while the samples analyzed with the Sonocat sensor are square elements measuring 50 × 50 cm.

For comparative analysis purposes, samples M35 and M45 were tested at 50 mm thickness, while samples K30 and K70 were tested at 40 mm thickness. This 20 % thickness difference (40 vs 50 mm) is

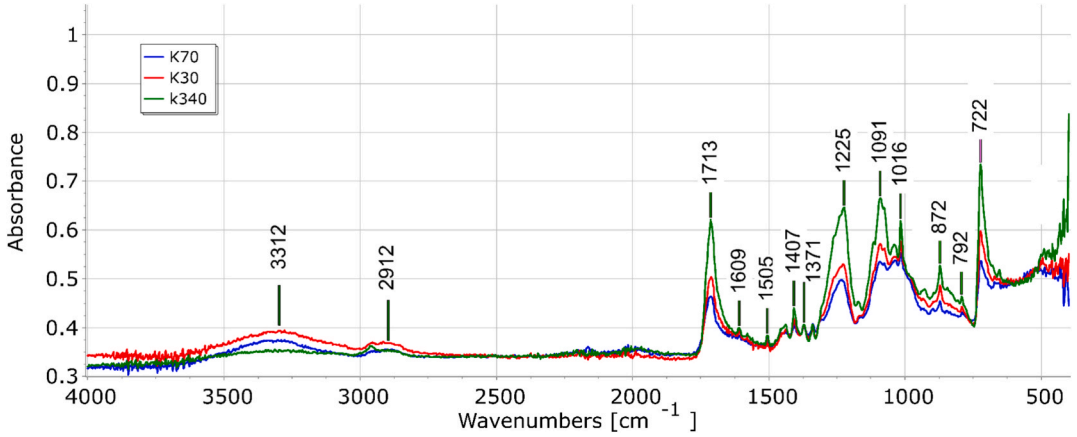

Fig. 7. IR spectra of the materials constituting the K30 (red), K70 (blue) and K340 (green) panels. For comparison, the spectra are baseline-corrected. (For interpretation of the references to colour in this figure legend, the reader is referred to the web version of this article.)

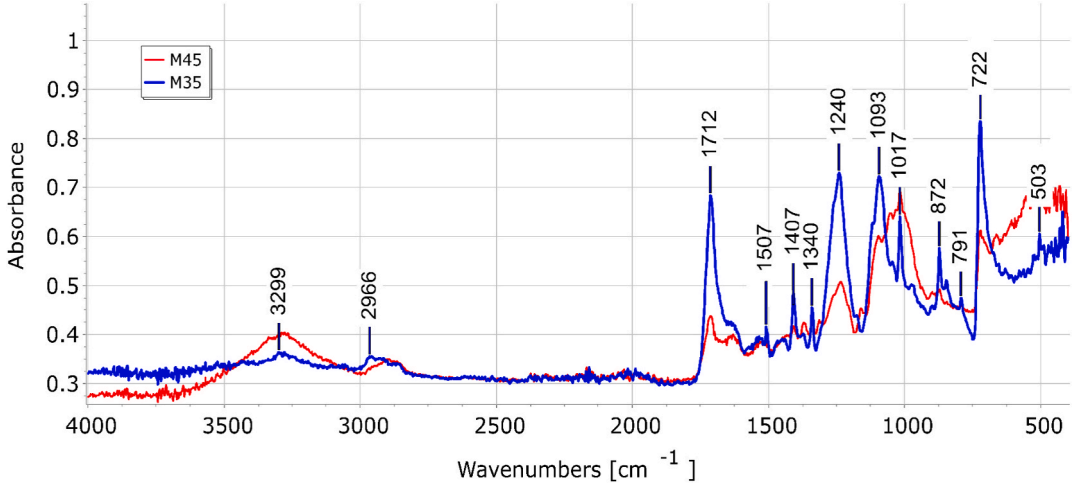

Fig. 8. IR spectra of the materials constituting the M35 (blue) and M45 (red) panels. For comparison, the spectra are baseline-corrected. (For interpretation of the references to colour in this figure legend, the reader is referred to the web version of this article.)

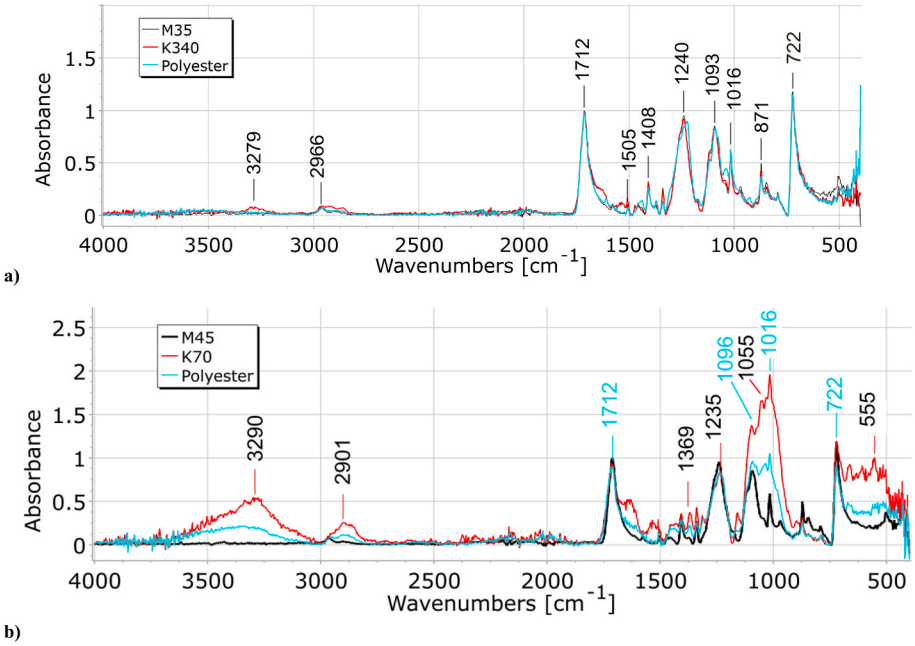

Fig. 9. Comparison of the IR spectra of polyester (azure) and the materials constituting **a)** M35 (blue) and K340 (green) panels with sample of polyester (azure) and **b)** M45 (red), K70 (blue) panels. The spectra are normalised on the intensity of the peak at 1712 $cm^{-1.}$ (For interpretation of the references to colour in this figure legend, the reader is referred to the web version of this article.)

considered acceptable for comparative acoustic analysis, as both thicknesses fall within the typical range for building insulation applications, and the variation is significantly smaller than other material-dependent factors. In contrast, sample K340 was specifically tested at 10 mm thickness to represent a different application scenario and demonstrates the substantial impact of thickness on acoustic properties. Due to this four-fold thickness difference, K340 data are analyzed separately and used primarily for illustrative purposes to highlight thickness-dependent effects rather than for direct material comparison.

Tests performed with the impedance tube

Tests on the same type of samples evaluate the measurement reproducibility, thus highlighting the eventual homogeneous composition of the panels.

Fig. 10 shows the acoustic properties measured for panels K made of hemp and kenaf. Samples K30 and K70 feature the same thickness of 40 mm, allowing for direct comparison of density effects, while K340 is 10 mm thick and serves to illustrate thickness-dependent behavior. As regards the sound absorption, K70 curves are shifted to lower frequency providing higher α values, behaviour in line with the effect of the higher density. Specimens K340 show the lowest α values, demonstrating how reduced thickness (combined with higher rigidity) significantly impacts acoustic performance. For what concerns the TL, the samples show a behaviour in line with their density and surface rigidity: higher is the density and higher is the TL.

Fig. 11 reports the acoustic properties measured for panels M made of textile. M35 and M45 samples have the same thickness (50 mm), but different density, enabling direct assessment of density effects on acoustic performance. Measured data show a higher variability than in the case of panel K, and this is probably due to the inhomogeneity of samples, as the panels are produced with different types of textile fibre. As previously seen, samples with higher density show higher α and TL

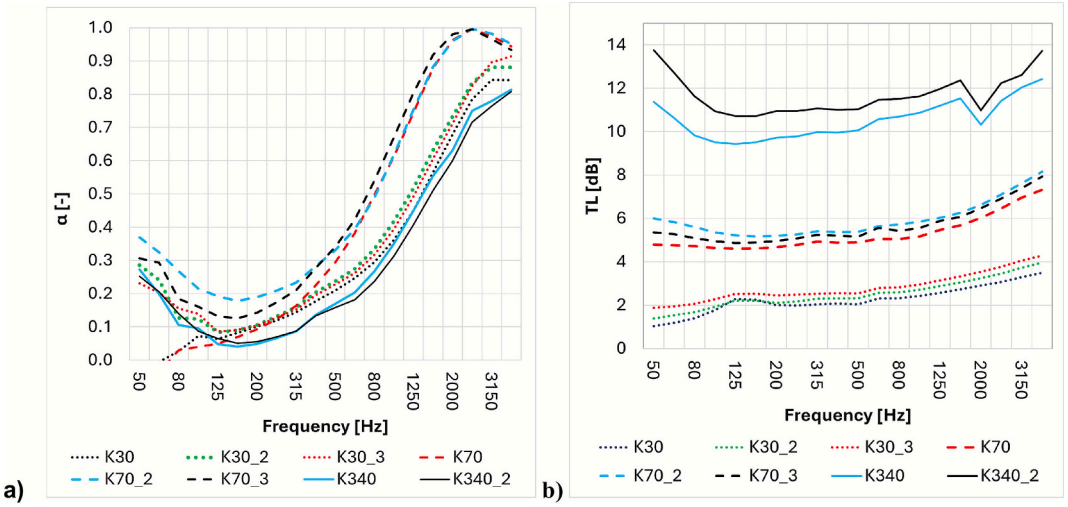

Fig. 10. Sound absorption α **(a)** and sound transmission loss TL **(b)** measured with the Kundt's tube for panels K made of hemp and kenaf.

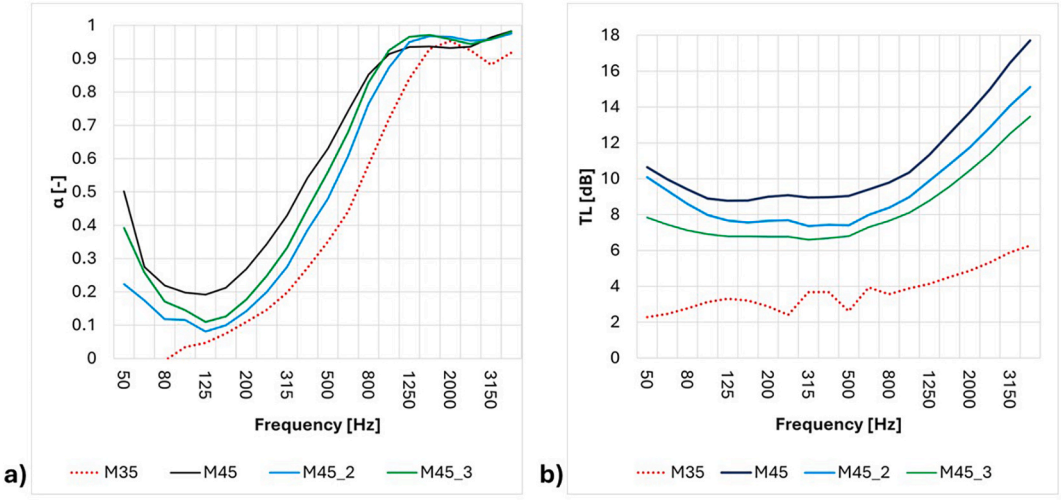

Fig. 11. Sound absorption α **(a)** and sound transmission loss TL **(b)** measured with the Kundt's tube for panels M made of textile.

values.

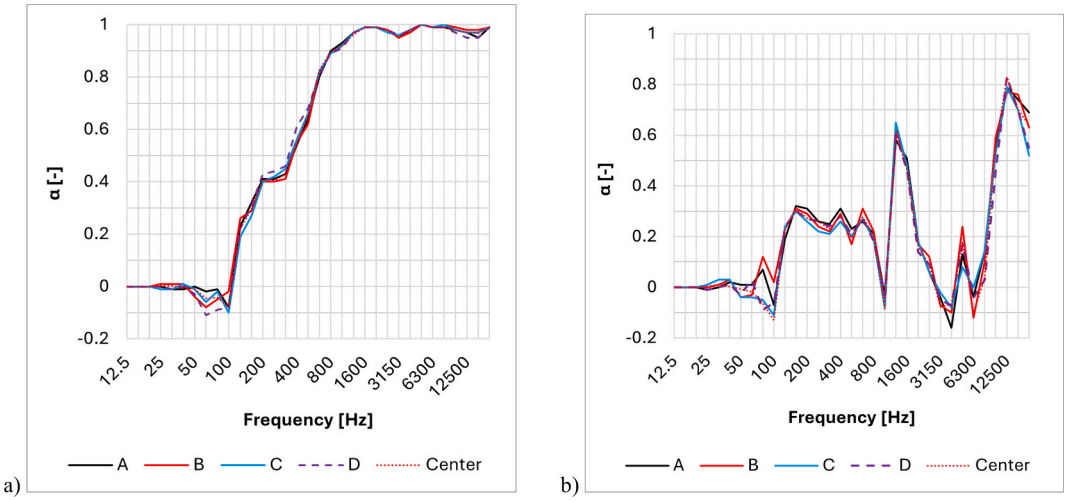

Fig. 12. Sound absorption coefficient α of known materials, the absorption material Basotect **(a)** and reflecting material EPS **(b)**, measured at different positions using the Sonocat sensor.

Sonocat tests

In this section, the results obtained from commercial materials derived from raw feedstock are first analyzed and serve as a benchmark for the analysis of the panels composed of recycled materials, which are the focus of this study.

Homogeneity of properties in EPS and Basotects panels (made from raw materials)

Basotect and EPS have been used as functional comparison materials and their experimental response has been evaluated. Values of α for Basotect panels are reported in Fig. 12 a). It shows excellent performance with absorption coefficients above 0.9 at frequencies over 1000 Hz, thanks to its highly porous structure that facilitates sound energy dissipation through viscous friction. The measurements demonstrated remarkable consistency across different sampling points, with minimal variation between the values measured at the center of the panel and those taken at surrounding points (A, B, C, D). This is an index of the material's highly homogeneous structure and consistent acoustic properties. Fig. 12 b) shows the results obtained for EPS. It is shown a limited absorption performance, attributable to the closed-cell structure of the material, which restricts sound wave penetration. The measurements show greater variability between center points and surrounding locations compared to Basotect, likely due to both the material's reflective properties and its less perfect homogeneity. However, these variations, while noticeable, remained within acceptable limits and did not significantly impact the overall characterization of the material's acoustic performance.

Homogeneity of properties in panels made from recycled materials

Fig. 13 shows α of panels M35 and M45 (both 50 mm thick). Panel M35 (Fig. 13 a) shows consistent repeatability at the same point (variations within 3 %) and comparable variability across different measurement points. Panels M45 (Fig. 13 b) demonstrates excellent overall repeatability, since a maximum variation in the absorption coefficient of less than 3 % has been observed in the four measurements taken at the same point. Measurements showed generally contained variability, with a maximum deviation of 4 % from the mean value. It is important to note that in the frequency range between 80 and 315 Hz, more significant variability was recorded in measurements taken at different points for panel M35. This phenomenon is primarily attributable to the nature of low-frequency sound waves, which have longer wavelengths and are therefore more sensitive to local variations in material structure and boundary conditions. Furthermore, in this frequency range, even small variations in density or local material compactness can significantly influence acoustic performance.

Results for panels K30, K70, and K340 are reported in Fig. 14. Measurements at the same point show good repeatability with variations within 3 %; however, measurements at different points revealed distinct behaviours. K30 showed more pronounced variability, particularly evident at low frequencies (80–315 Hz), likely due to the material's low density. The more compact structure of panel K70 ensures more uniform performance throughout the sample. Panel K340, with its significantly reduced thickness and consequent high rigidity, shows distinct acoustic behavior and some variability in measurements at different points, highlighting how thickness substantially affects both performance magnitude and measurement consistency.

Comparison of performance between panels made from raw and recycled materials

The comparison of the sound absorption coefficient α measured for the different panels is reported in Fig. 15. This comparative analysis focuses primarily on samples with similar thicknesses (M35/M45 at 50 mm, K30/K70 at 40 mm), while K340 (10 mm) serves as an illustrative example of thickness-dependent effects. It is reminded that the two materials used as functional benchmarks have different thicknesses, that is Basotect panel is 50 mm thick, while EPS panel is 60 mm thick.

The results for the M45 recycled textile panel are particularly noteworthy. The measurements, which show remarkable agreement between the Kundt's tube and the Sonocat probe, indicate excellent performance with an α comparable to that of Basotect above 1000 Hz. This finding is consistent with the scientific literature on textile-based insulators, where high absorption coefficients in the mid-to-high frequency range are often reported and attributed to the material's high porosity and tortuosity. The performance of the M45 panel positions it as a competitive and sustainable alternative to traditional synthetic materials. The M35 panel, while showing slightly lower performance at high frequencies, exhibits an interesting behavior in the 315–400 Hz range, where it outperforms the denser M45 version. This phenomenon, contrary to the theoretical expectation that higher density should lead to greater absorption, could be attributed to fiber resonance within a less compact structure. This aligns with findings for other fibrous materials, which suggest that an optimal density, rather than the maximum possible, often exists to maximize absorption by balancing airflow resistivity and porosity.

Regarding the kenaf and hemp panels (K30 and K70), the analysis reveals that K70 emerges as the most balanced solution, achieving significant performance at high frequencies. This is in line with literature indicating that for natural fibers, an increase in density generally improves acoustic absorption across a broad frequency spectrum. On the other hand, the K30 variant is more effective in the 100–400 Hz range,

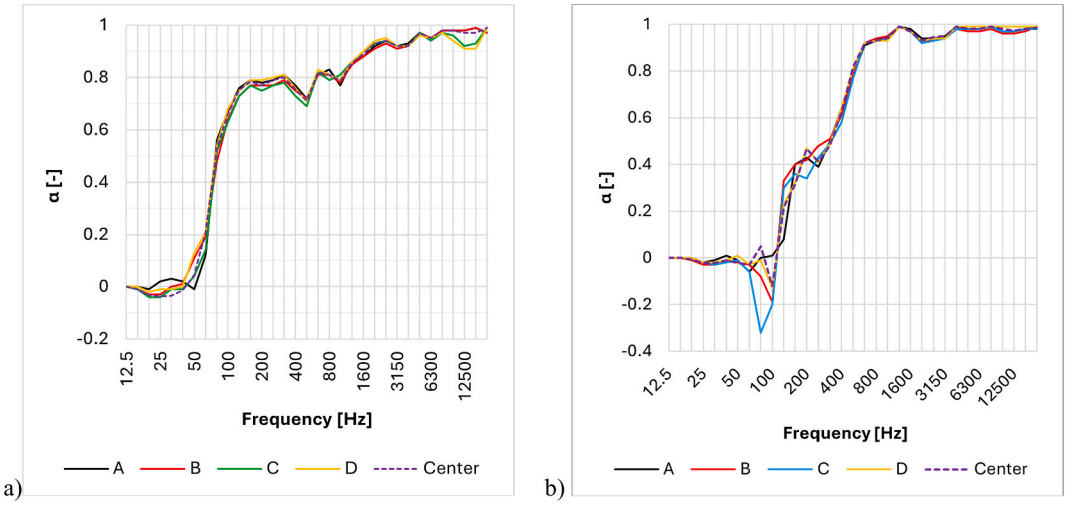

Fig. 13. Sound absorption coefficient of standard commercial insulating materials, M35 **(a)** and M45 **(b)**, measured at different positions using the Sonocat sensor.

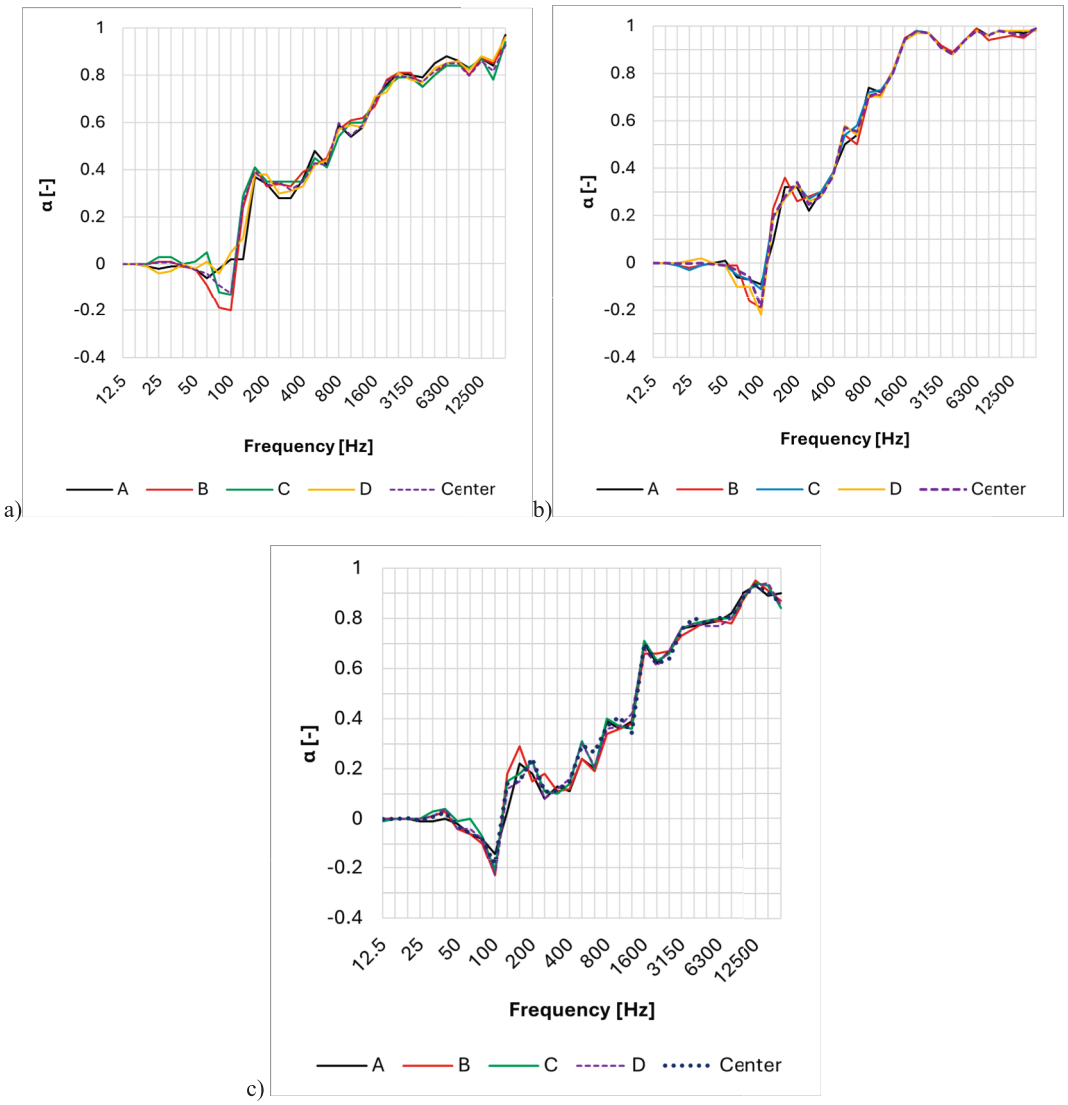

Fig. 14. Sound absorption coefficient of standard commercial insulating materials K30 **(a)**, K70 **(b)**, and K340 **(c)** measured at different positions using the Sonocat sensor.

where it surpasses the denser versions. This behavior suggests that low-density panels could be better suited for applications targeting low-frequency attenuation. Despite the different panels thickness, the comparison with the K340 panel (10 mm) clearly demonstrates how significantly reduced thickness and consequent high rigidity drastically compromise acoustic performance, a fundamental principle widely documented in the acoustics of porous materials.

To provide a standardized, single-number metric for practical comparison, the Noise Reduction Coefficient (NRC) was calculated for each material. It is important to contextualize the utility of the NRC. While this single-number rating offers a convenient overview of a material's general sound-absorbing potential, it is an average across a limited frequency range (250–2000 Hz). For detailed acoustic design, a material's suitability is best determined by analyzing its full absorption curve, as presented in Fig. 15. The complete curve is crucial because a material might have a high NRC but perform poorly at the specific frequencies that need to be attenuated for a particular application. Therefore, while the NRC value gives a good initial idea of the material's potential, the full frequency response remains the essential tool for effective and targeted acoustic treatment. The recycled textile panels demonstrated outstanding performance, with the M35 achieving the highest NRC of 0.80, closely followed by the M45 at 0.77. These values confirm their potential as high-performance broadband absorbers. The kenaf/hemp panels showed a clear progression, with the K70 panel registering a respectable NRC of 0.63, while the K30 scored 0.52, respectively. The K340 variants showed a NRC of only 0.35, probably due to the limited thickness of the tested panel.

In summary, these results confirm that density is a crucial parameter for optimizing acoustic performance. Panel K70 represents the best compromise among the hemp/kenaf variants, offering competitive performance. Meanwhile, M45 has proven to be a promising sustainable alternative to Basotect, especially for high-frequency applications. The performance differentiation between the two textile panels (M35 and M45) allows for targeted material selection based on specific acoustic goals. The superior broadband performance of the less-dense M35, reflected in its slightly higher overall NRC, highlights a complex, non-linear relationship between density and absorption in these recycled textile composites that warrants further investigation.

To provide a comprehensive comparison with existing literature, the SAA values obtained in this study were benchmarked against recent research on sustainable acoustic panels. In (Hassani et al., 2024), it is reported SAA values ranging from 0.17 to 0.60 for panels fabricated from recycled discarded denim with varying densities (80–140 kg/m^3) and thicknesses (0.01–0.05 m), with optimal performance achieved at

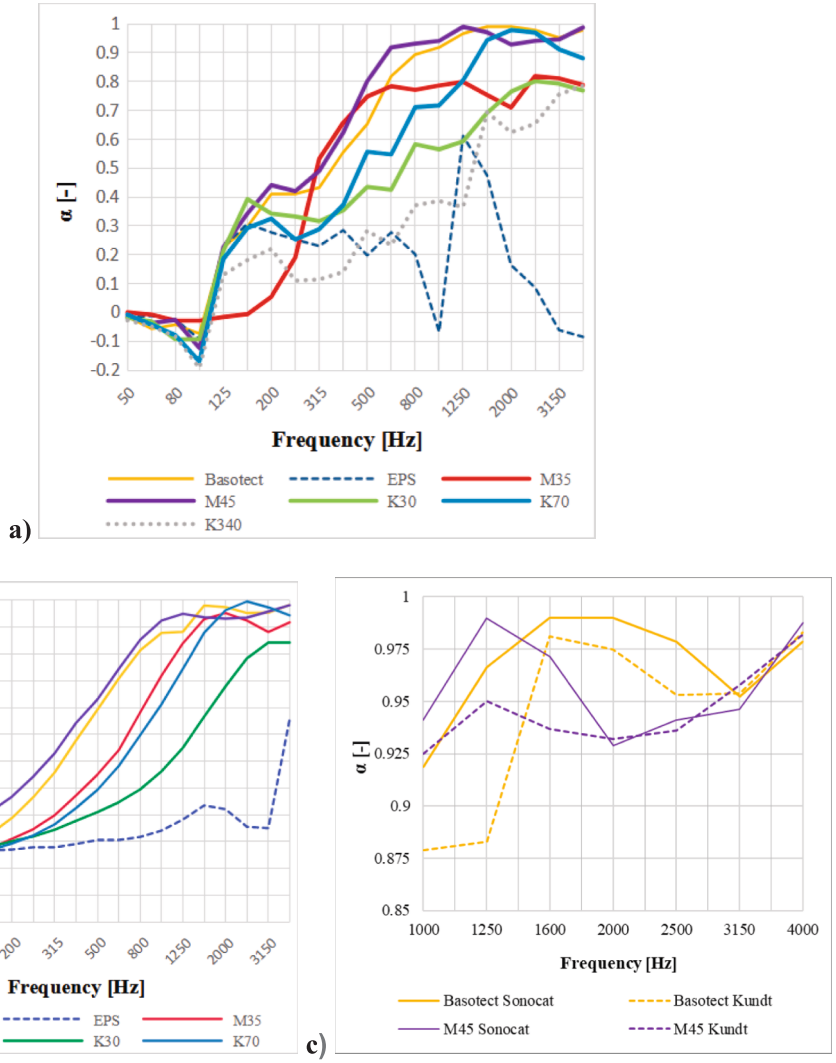

Fig. 15. Comparison of the sound absorption coefficient measured with Sonocat **(a)**, the Kundt's tube **(b)** for the different materials, and **(c)** comparison of the results above 1000 Hz obtained for Basotect and M45. It is reminded that K340 has a very different thickness and therefore a direct comparison is not possible; anyway it is reported to make a general comparison of all the tested samples. For the other samples, the thickness is 50 mm for M35, M45 and Basotect; 40 mm for K30 and K40; and 60 mm for EPS.

0.538 under controlled conditions. Furthermore, in (Halashi et al., 2024) luffa fiber panels were examined and found SAA performance ranging across different frequency bands, with enhanced absorption in the critical indoor frequency range of 500–2000 Hz. These studies collectively demonstrate that sustainable bio-based and recycled materials can achieve competitive acoustic performance, with SAA values typically ranging between 0.15 and 0.65 depending on material density, thickness, and structural configuration.

The authors acknowledge that all panels tested originate from a single manufacturer, and composition variability – particularly evident in the M−series through FT-IR analysis – represents a limitation for generalizability. The inherent variability in recycled textile waste streams means that composition can differ between production batches and manufacturers. However, several findings can be considered broadly applicable. In particular, the correlation between acoustic behavior, density, and thickness is expected to remain valid across different manufacturers, since it reflects fundamental physical principles rather than brand-specific characteristics. Likewise, the greater compositional uniformity observed in Kenaf-based panels—confirmed through FT-IR analysis—translates into more predictable acoustic performance, highlighting an intrinsic advantage of single-source natural fibers. Furthermore, the measurement methodologies adopted and the analytical framework developed are fully transferable to other contexts, ensuring that the approach can be replicated beyond the present case study. At the same time, certain aspects remain closely tied to the specific suppliers examined and therefore require further validation. These include the absolute acoustic performance values measured for the M−series panels, the precise composition ratios identified through FT-IR, and the degree of batch-to-batch variability observed in recycled textile panels. To consolidate these insights, future work should involve multi-supplier testing. Such comparative analyses will help establish reliable performance ranges and clarify which compositional parameters most critically influence the acoustic behavior of recycled textile insulation materials.

Measurement uncertainty and method comparison

The reliability of acoustic characterization depends critically on understanding the uncertainty associated with each measurement method. In this study, both standardized (impedance tube) and innovative (Sonocat) techniques were employed, each exhibiting distinct uncertainty characteristics that reflect their different operational principles and measurement conditions.

Impedance tube measurements demonstrated excellent repeatability owing to the controlled laboratory environment and standardized ISO

10534–2 (International Organization for Standardization, 2023) procedure. For each panel typology, three samples extracted from different positions were tested, with each sample undergoing three repeated measurements. The resulting absorption coefficient curves represent the average of these nine total measurements (3 samples × 3 repetitions), yielding a remarkably low standard deviation of 0.001. This precision is attributable to the elimination of external variables, stable environmental conditions, and the use of calibrated instrumentation within a confined acoustic system. The frequency-dependent behavior across the measured range (50–4000 Hz) showed consistent patterns, with negligible variation between repetitions at the same measurement point. This level of precision enables direct comparison with literature data and provides a reliable baseline for material characterization.

Sonocat measurements, while operating in a less controlled environment, provided valuable insights into real-world material performance with quantifiable uncertainty bounds. Repeatability at the same measurement point was excellent, with variations contained within 3 % across multiple acquisitions. However, spatial variability—inherent to any in-situ measurement on larger specimens—was more pronounced, particularly at low frequencies (80-315 Hz) where the longer wavelengths are more sensitive to local material heterogeneities, edge effects, and mounting conditions. Measurements at different locations (center and four peripheral points A, B, C, D) showed a maximum deviation of 4 % from the mean value across the mid-to-high frequency range. This spatial variability is not measurement error per se, but rather reflects genuine material inhomogeneity and the influence of boundary conditions that would be present in actual applications. The contained magnitude of this variability ($\leq$ 4 %) confirms both the material's acceptable homogeneity and the Sonocat's capability to capture realistic performance variations.

The frequency-dependent uncertainty deserves particular attention, as the SAA metric, while useful for single-number comparison, inherently masks important spectral behavior. At low frequencies (80–315 Hz), both methods showed increased variability: the impedance tube due to the approach to the lower measurement limit, and the Sonocat due to the combined effects of probe size limitations and material wavelength-sensitivity. Conversely, in the mid-frequency range (400–2000 Hz)—most critical for building acoustics—both methods demonstrated their best performance with minimal uncertainty and excellent mutual agreement. This frequency-specific characterization provides designers with the confidence intervals necessary to make informed material selections for specific acoustic applications.

The dual-method approach adopted in this study thus provides complementary information: the impedance tube offers high-precision, repeatable data ideal for quality control and inter-laboratory comparison (uncertainty ~ 0.1 %), while the Sonocat reveals realistic performance variability under application-relevant conditions (spatial uncertainty ~ 3–4 %). This combination enables both rigorous material characterization and practical performance prediction. Beyond individual method uncertainty, a critical question concerns the systematic agreement between impedance tube and Sonocat measurements. Given the fundamental differences in measurement principles—normal incidence in a controlled tube versus quasi-diffuse field in situ—perfect agreement is neither expected nor physically meaningful. However, understanding the nature and magnitude of any systematic bias is essential for interpreting results.

A direct comparison of absorption coefficients measured by both methods reveals consistent patterns across all tested panels. In the mid-to-high frequency range (500–4000 Hz), where both methods operate within their optimal domains, the agreement is remarkable, with typical differences $\Delta\alpha(f) = |\alpha\_Sonocat(f) - \alpha\_tube(f)|$ remaining below 0.05 for most materials. This close correspondence validates both the material homogeneity and the measurement reliability. For the M45 panel, which showed the best performance, the two methods produced nearly overlapping curves above 1000 Hz, with $\Delta\alpha(f) < 0.03$ across this range, demonstrating excellent mutual validation. At low frequencies (80–400 Hz), systematic differences become more apparent, with the Sonocat generally measuring slightly lower absorption coefficients than the impedance tube. This bias is physically interpretable: the impedance tube measures normal incidence absorption under ideal plane-wave conditions, while the Sonocat operates in a more complex sound field that better represents diffuse building acoustics conditions. The observed $\Delta\alpha(f)$ in this range (typically 0.05–0.15) is consistent with the well-documented difference between normal and random incidence absorption coefficients for porous materials, where random incidence values are typically lower, particularly at frequencies where the material thickness is small relative to wavelength.

Importantly, no evidence of random, unsystematic discrepancies was observed—the differences between methods follow predictable, frequency-dependent patterns that align with acoustic theory. The impedance tube consistently provides the upper bound (normal incidence), while the Sonocat provides a more conservative estimate representative of real-world diffuse conditions. This systematic relationship, rather than being a limitation, actually enhances the value of the dual-method approach: designers can use the impedance tube data for standardized comparisons and the Sonocat data for realistic performance predictions, with the understanding that actual building performance will typically fall between these bounds.

For the recycled textile panels (M35, M45), the excellent agreement at application-relevant frequencies (400–2000 Hz) confirms that these materials perform consistently under both idealized and realistic conditions, supporting their viability as sustainable acoustic solutions.

Fire response of the materials

Ignition temperature and produced gases

Figs. 16 and 17 report typical profiles obtained in the TPO experiments, whereas the quantitative data are summarized in Table 2.

Fig. 16 refers to panels M35 and M45 which show comparable behavior upon heating in air. Two prominent and partially overlapped peaks can be identified both for CO and CO_2, with maxima at ca. 445 °C and 530 °C for M35, and 370 °C and 505 °C for M45. The amount of CO_2 produced accounts for about 64–68 % of the evolved gases, indicating a non-complete combustion during the TPO experiment, consistent with real fire conditions. As for the other species detected, only acetaldehyde forms have significant amounts, up to 7 % in sample M35 compared to 1.9 % in M45, whereas all the other species are less than 1 % of the overall gas evolution. Also, the overall amount of the evolved gases is significantly different between M35 and M45 samples. Given the relatively small difference in the panel density, such differences could be related to the different nature of the fibers, as detected by the FT-IR technique.

The TPO profile for the K samples is shown in Fig. 17. The TPO appears somewhat different compared to the M samples: even if there are still two peak patterns, the relative intensity of the CO_2/CO peaks at low temperature is significantly lower compared to those at high temperature. The peak at 460 °C – 484 °C is very sharp and accounts for most of the evolved gas. Noticeably, the temperature profiles feature a clear exothermal phenomenon in correspondence of the major peak, which is associated with ignition and burning of the material during the TPO experiment. Consistently, the total amount of CO_2/CO evolved in samples K is in the range 94–98 % compared to 87–88 % in the panels M, suggesting a higher flammability of the former samples.

According to Table 2, the total volume of gas evolved during thermal decomposition of K samples decreases significantly with the sample density. Likewise, as the density of panels K increases, the decomposition temperature moves to higher temperatures, both effects suggesting that carbonisation is favoured as the sample density increases. Consistently, black deposits are found at the outlet of the TPO reactor.

Effect of the fire retardant

Whereas the effects of the fire-retardants are not the main focus of

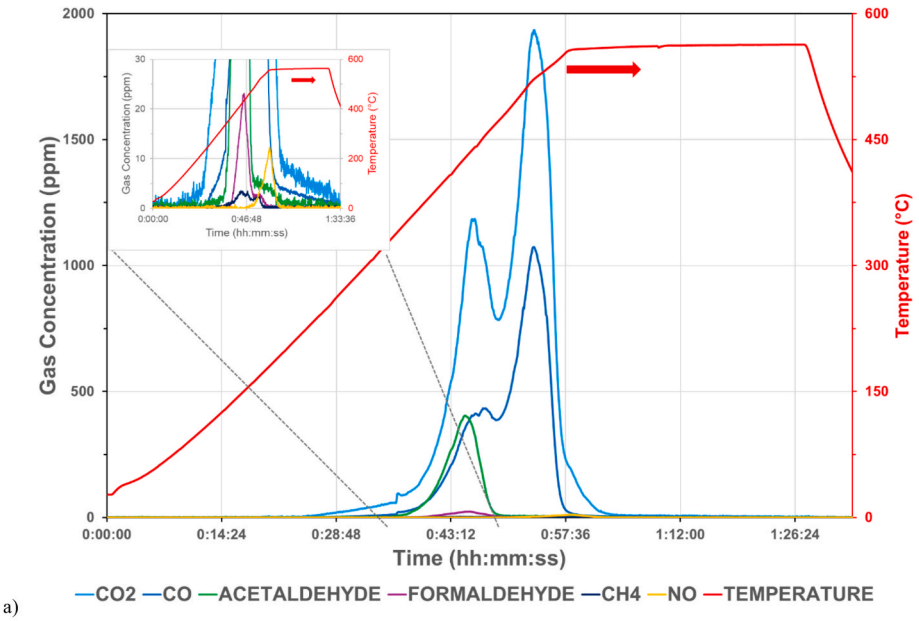

a)

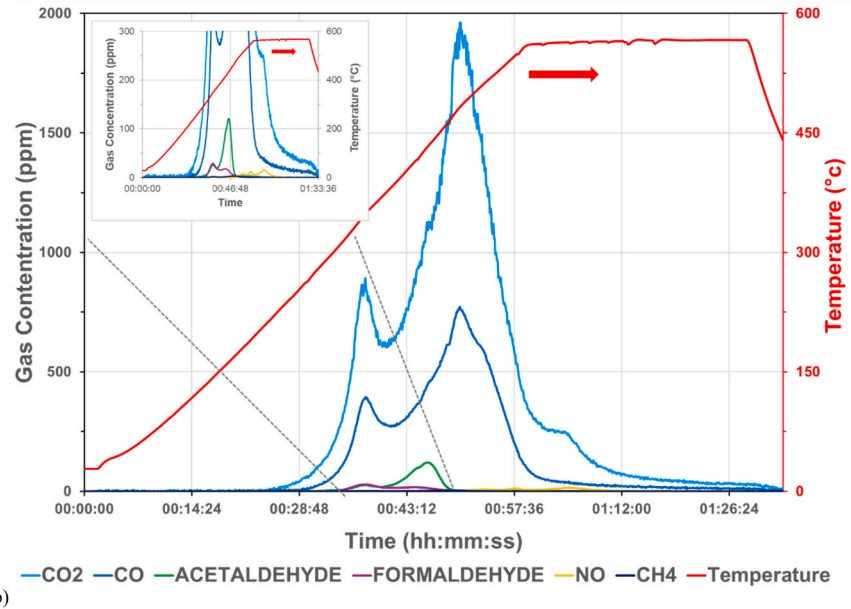

b)

Fig. 16. TPO profiles obtained for panel **(a)** M35 and **(b)** M45. The CO_2, CO and other gases concentration (ppm, left axis) detected during the thermal decomposition of the material and the temperature profile (°C right axis) are plotted as a function of reaction time. In the inset of the enlargement the gases evolved in low concentrations.

this work, due to the potential high flammability of natural fibres, we included some data concerning the K30 sample as an example of the effects, since it shows the highest ignitability as denoted by its low ignition temperature. Firstly, the thermal decomposition of solid FR was first analyzed which, according to Fig. 18, results in the significant formation of CO_2 and NH_3, which act as primary FRs. Both gases are non-flammable, and NH_3 in the considered temperature range reduces the concentration of oxygen in the environment, which contributes to preventing the sample ignition. It is worth noting that a small quantity of isocyanic acid was detected, which is toxic and can cause asthma, inflammation of the respiratory tract, and cancer (Bengtström et al., 2016).

Fig. 19 shows the results obtained for the K30 samples treated with the FR. Noticeably, the panels do not ignite, indicating that the FR promotes char formation rather than combustion. However, the decomposition of the FR resulted in the production of ammonia and isocyanic attributable to the decomposition of FR since it was not detected for the untreated K30. Consistently, the volume of ammonia in the experiment with the K30-FR1.8 % sample was significantly smaller than in the K30-FR13% sample, as reported in Table 2. The profile evolution of the gases differs between the FR-treated K30 samples and the untreated one, indicating that the FR has a significant impact on the decomposition process of the K30 sample.

Fig. 20 compares the evolution of CO_2 and NH_3 gases in the TPO experiments carried out on the solid FR and the two treated K30 samples. A perusal of Figs. 19 and 20, reveals that the pattern of the decomposition is markedly distinct in the treated and untreated samples, particularly with regard to peak maximum and gas amount. The quantity of ammonia evolved in the K30 sample treated with a diluted solution is far less than that evolved in the K30 sample treated with a pure solution of FR. Moreover, the ammonia evolution temperature in solid and the treated FR samples exhibits notable differences, which can be

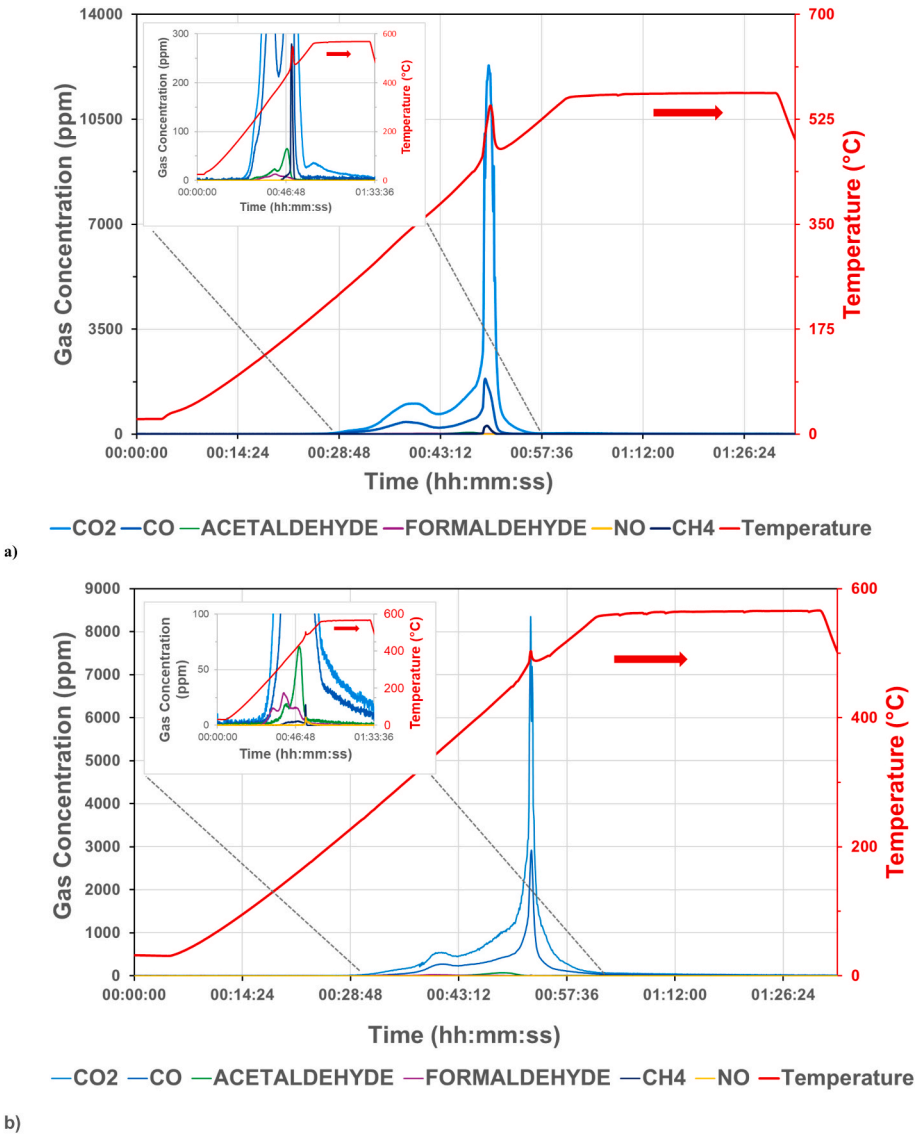

Fig. 17. TPO profiles obtained for materials **a)** K30, **b)** K70, and **c)** K340, during the TPO experiments. The CO_2, CO and other gases concentration (ppm, left axis) detected during the thermal decomposition of the material and the temperature profile (°C right axis) are plotted as a function of reaction time. In the inset of the enlargement the gases evolved in low concentrations.

attributed to a chemical interaction between the FR and the compounds of the natural fibres. Finally, the quantity of isocyanic acid evolved during the decomposition of the treated samples is minimal. Even if it is a toxic gas, this appears not to be a significant issue in the thermal decomposition of the FR when used in an insulation panel, particularly if it is loaded in a low concentration where still effective for eliminating the ignition phenomenon of the materials.

The volume of evolved gas from the sample treated with the diluted solution of FR increases compared to sample K30-FR13%, which could be attributed to a lower amount of FR, which is responsible for additional – compared to K30 – NH_3 and CO_2 volume. Nevertheless, even the treatment with a diluted solution is effective in eliminating the ignition phenomenon of the sample. To ensure that the observed effects were not due to immersion in an aqueous solution, a blank experiment was conducted with a water-only treated K30 sample; in this case ignition occurred and the decomposition pattern of the gases was similar to that of the untreated sample, thus confirming the important role of the FR in the fire resistance even for low FR loading. The low "decomposition" temperatures reported for the FR-treated samples are associated with the decomposition of the impregnated FR.

In summary, the analysis of thermal properties and fire resistance of the insulation panels revealed that sample density plays a key role in material behaviour. Higher-density samples exhibited lower ignition potential and reduced gas emissions during thermal decomposition, likely due to decreased oxygen interaction, which inhibits carbonization. This pattern was observed for panels K samples but not in panels M, where variations were linked to different compositions. Additionally, the fire retardant (FR) treatment of the K30 sample significantly altered its degradation, eliminating ignition and reducing gas production even at low concentrations of FR. These findings are especially relevant, as smoke inhalation is a major cause of fatalities in fire accidents.

The experimental results reported in this paper confirm the potential of natural and recycled fibre panels for thermal and acoustic insulation. However, broader considerations are essential to evaluate their real-world applicability. Durability remains a critical issue since these materials may be vulnerable to moisture and biological degradation over time. Long-term performance testing under varying environmental conditions is necessary. From a sustainability perspective, these

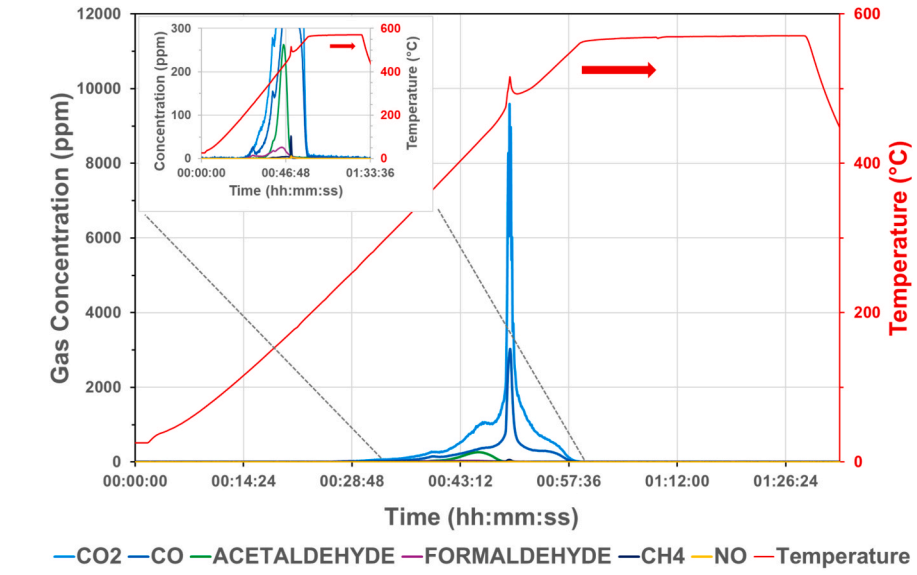

c)

Fig. 17. (*continued*).

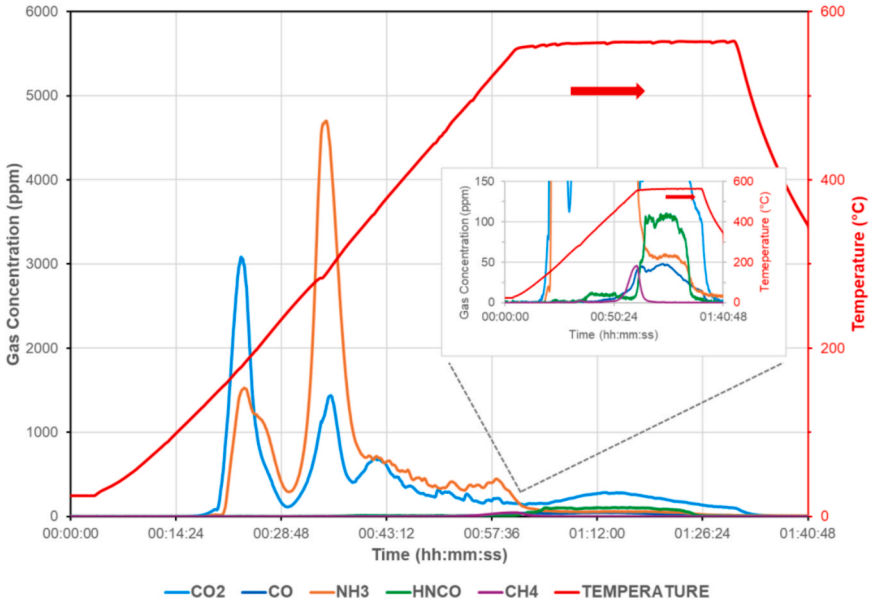

Fig. 18. TPO profile obtained for solid FR. The CO_2, CO, and other gas concentrations (ppm, left axis) detected during the thermal decomposition of the material and the temperature profile (° C right axis) are plotted as a function of reaction time. In the inset of the enlargement the gases evolved in low concentrations.

materials align with circular economy goals, offering alternatives to fossil-based products and reducing textile and agricultural waste. The IR analysis reveals, however, that use of recycled materials is prone to difficulties as far as the reproducibility of the product concerns, due to the variable textile waste composition, leading to samples with different properties. Nonetheless, a full life cycle assessment (LCA) would be needed to quantify their environmental impact from production to disposal. Cost feasibility is promising, particularly for applications in low-income contexts. However, the variability in composition—especially in textile-based panels—could hinder scalability and standardization, posing challenges for consistent performance. In terms of regulatory compliance, current fire classifications (E–F) limit their use in many buildings. Even with fire-retardant treatments, the release of potentially harmful gases raises concerns that must be addressed through improved formulations and further safety testing. Additionally, the lack of standard certification pathways (e.g., CE marking) remains a barrier, especially for recycled materials. Overall, while these panels show encouraging performance, integration into the construction market will require advancements in durability, regulatory alignment, and quality control, along with further research on environmental and economic impacts. Their development supports a more inclusive and sustainable construction sector but must be guided by robust validation frameworks.

Conclusions

Insulating panels made from recycled or organic materials are gaining increasing attention due to their alignment with the principles of

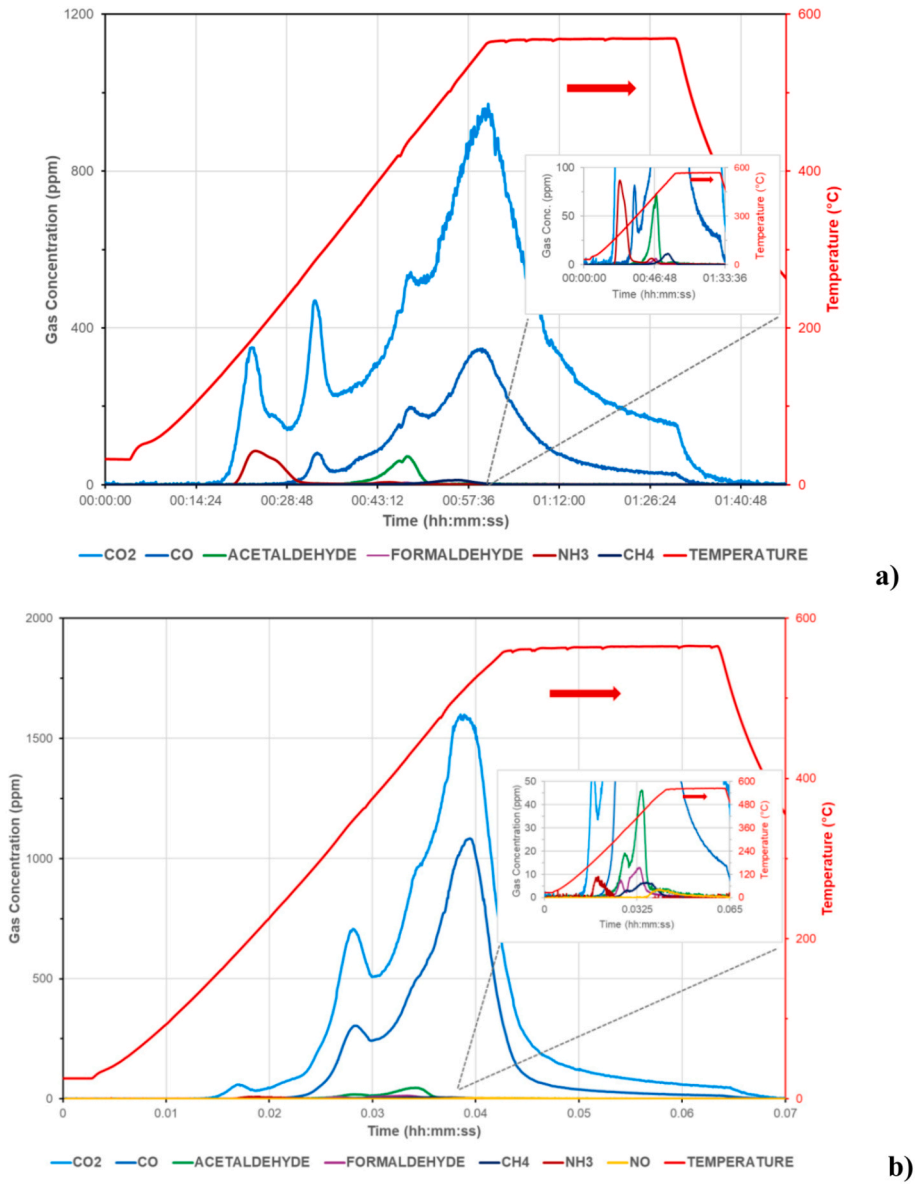

Fig. 19. Results of TPO experiments of K30-FR13% **a)** and K30-FR1.8%, **b)** CO_2, CO, NH_3 and other gases evolved during the thermal decomposition of the compound. In the inset of the enlargement the gases evolved in low concentrations.

the circular economy. However, compared to conventional insulating materials, they present certain challenges – particularly regarding the consistency of their properties, which is influenced by the collection and sorting methods of secondary raw materials. The complexity of the sorting process and the wide variety of usable fibers make standardization a goal that remains difficult to achieve.

This study analyzed two types of commercially available panels, subjecting them to both standardized tests and custom-designed experimental protocols, with the aim of assessing compositional and performance variability. After identifying structural and functional limitations, special focus was placed on improving fire behavior—one of the main hurdles for large-scale application. The research went beyond established methodologies by introducing unconventional testing procedures to explore aspects related to composition, thermal and acoustic properties, and fire response. The results provide concrete insights for optimizing sustainable insulating panels, contributing to their advancement in terms of performance and applicability. In particular, the study analyzes the properties of panels made from recycled textiles (panels M) and natural fibers of kenaf and hemp (panels K), bonded with polyester. The study aimed to evaluate the homogeneity of properties across the panel surfaces, focusing on composition, measured density compared to the one declared by the manufacturer, thermal conductivity, and acoustic properties. Moreover, it has been investigated the fire behaviour of the panels focusing on the quantity and quality of gas produced when exposed to high temperature. Also, the effects of a fire retardant have been evaluated considering different dilution percentages. The main findings can be summarized as follows:

- Regarding the panels composition and the declared density, panels M exhibit greater variability. This inconsistency stems from the diverse sources of textile fibers, which are a mix of the products available. This result confirms that textile fibers are difficult to sort and standardize. Conversely, kenaf-hemp panels displayed greater uniformity, making them more predictable in terms of properties.
- Regarding the thermal conductivity, values for the panels ranged between 0.035 and 0.049 W/(m·K). Material M panels exhibited greater variability in the results, whereas values obtained for material K showed a decreasing trend in thermal conductivity with

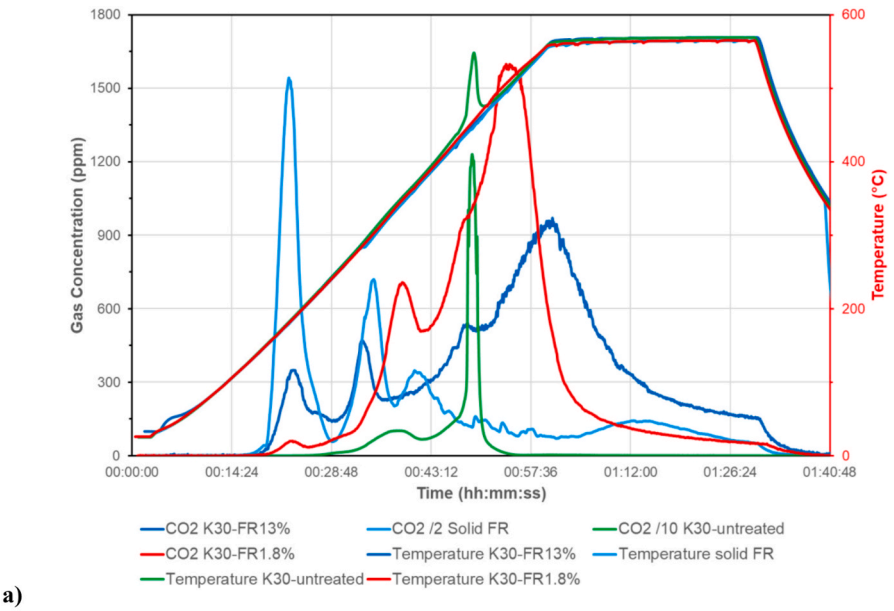

a)

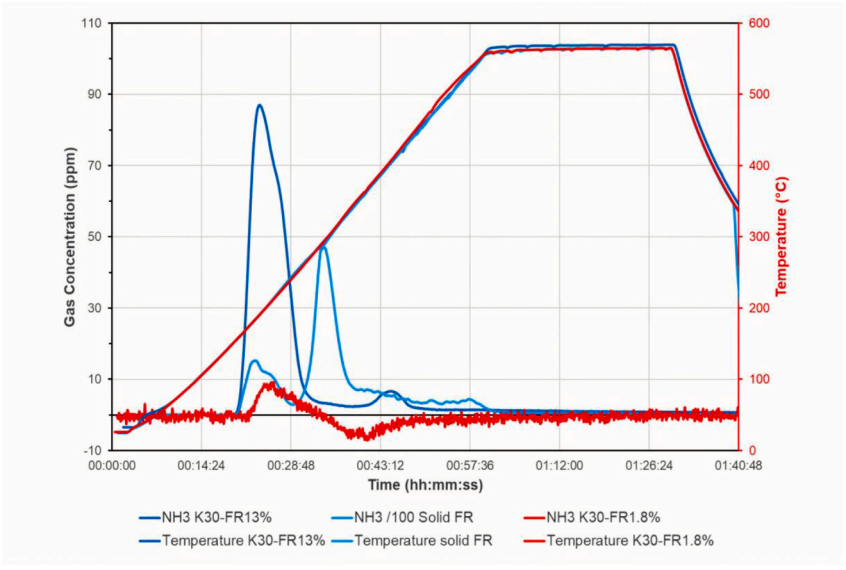

b)

Fig. 20. Comparison of **a)** CO_2 and **b)** NH_3 evolution during experiment with solid FR (light blue), K30-FR13% (blue), K30-1.8% (red) and K30 untreated (green). Note that the concentration is divided by 2 and 10 in Solid FR and K30 untreated respectively in a), and by 100 in Solid FR in b). (For interpretation of the references to colour in this figure legend, the reader is referred to the web version of this article.)

increasing density. This behaviour is consistent with the U-shaped trend of conductivity as a function of density, observed in several insulating materials used in construction.

- Regarding the acoustic properties, this study provides a significant contribution to the field of sustainable building materials by validating recycled textiles as a high-performance acoustic material and analyzing the nuanced effects of density and material variability. A primary finding is the quantitative demonstration that the M45 recycled textile panel achieves a sound absorption performance ($\alpha >$ 0.9 above 1000 Hz) directly comparable to Basotect, a high-performance commercial benchmark. This not only confirms the potential of textile waste as a viable raw material but also positions these panels as a competitive, sustainable alternative for demanding acoustic applications—an aspect not extensively explored in direct comparison with commercial benchmarks. Furthermore, the work reveals a complex relationship between density and acoustic performance, contributing new empirical evidence to the discussion on material optimization. While for the kenaf/hemp panels (K-series) a higher density (K70) improves transmission loss (TL) and provides balanced absorption. A non-linear behavior is observed for the textile panels (M−series), where the less dense version (M35) outperforms the denser one (M45) at mid-frequencies. This suggests that finer fiber composition influences the acoustic response in ways that differ from standard theoretical expectations. Finally, the study addresses the practical challenge of material consistency. By using two complementary measurement techniques, it quantifies the greater variability in the acoustic properties of panels derived from recycled textiles (M) compared to those from natural fibers (K). This is a crucial contribution for the industrial-scale adoption of these materials, as it highlights the need to develop standardization processes for textile waste streams to ensure reliable performance – a key challenge noted in the literature on the circular economy in construction. Taken together, these results not only characterize novel materials but also provide a scientific basis for their market positioning, highlighting both their technical potential and the

standardization challenges that must be addressed for their widespread adoption.

- Regarding the fire response of the material during the TPO test, panels M35 and M45 did not undergo complete combustion. The amount of CO_2 produced ranged from 64 % to 68 %, while acetaldehyde was the only other gas released in notable quantities. A distinct exothermic reaction was observed in the kenaf-based panels (K-series), indicating ignition and sustained combustion. This suggests that kenaf-based panels not only exhibit higher flammability compared to those made from textile fibers, but in the case of fire accidents they possibly would spread and propagate the fire. Additionally, the total volume of gases evolved during decomposition decreased significantly with increasing sample density. Higher density samples also exhibited a shift in decomposition temperature to higher values: for instance, K30 ignited at 460 °C, while K70 ignited at 484 °C. These findings indicate that increased density promotes carbonization over combustion.
- Regarding the effects of the fire-retardant treatments, the retardant-treated panel K30 exhibited enhanced char formation rather than combustion. Even treatment with a dilute solution proved effective in suppressing ignition. However, gas analysis revealed the presence of certain toxic decomposition products—such as ammonia and isocyanic acid—in the treated samples, albeit at low concentrations, which can affect the degree of toxicity of the evolved gases. On the other hand, even low concentrations of the deposited fire-retardant effectively suppress the exothermic phenomena of the untreated samples which would mitigate spreading and propagation of the fire. Thus the TPO technique appears to effectively provide information on the toxicity of gases evolved in a fire accident that involves the insulating material. These aspects will be discussed in a forthcoming paper.

The main innovative contribution of this research lies in the adoption of a multidisciplinary and non-conventional approach, which through alternative techniques (actual vs declared density, IR spectroscopy, Sonocat, TPO) enabled the identification of properties of natural and recycled fiber panels not detectable with standardized tests, and positioned them within a comprehensive comparative framework against acoustic reference extremes. The results obtained are valid for the cases analyzed and, although they cannot be generalized to all manufacturers, it is considered that they may be extended to other production contexts: this does not imply that all materials present the same critical issues, but highlights that the problem identified is real and deserves attention with a view to broader adoption.

CRediT authorship contribution statement

Jan Kašpar: Writing – original draft, Supervision, Resources, Project administration, Methodology, Funding acquisition, Formal analysis, Data curation, Conceptualization. **Giada Kyaw Oo D'Amore:** Writing – original draft, Investigation, Formal analysis, Data curation. **Jessica Ferrari:** Writing – original draft, Formal analysis, Data curation. **Enrico Armelloni:** Methodology, Investigation, Data curation. **Vincenzo Ballerini:** Formal analysis, Data curation. **Paolo Valdiserri:** Writing – original draft, Supervision, Resources, Data curation. **Eugenia Rossi di Schio:** Writing – original draft, Supervision, Resources, Project administration, Funding acquisition, Data curation. **Mariagrazia Pilotelli:** Writing – original draft, Supervision, Resources, Project administration. **Hossein Soltanian:** Writing – original draft, Data curation. **Manuela Neri:** Writing – original draft, Supervision, Project administration, Funding acquisition, Conceptualization.

Funding

We acknowledge financial support under the National Recovery and Resilience Plan (NRRP), Mission 4, Component 2, Investment 1.1, Call for tender No. 104 published on 2.2.2022 by the Italian Ministry of University and Research (MUR), funded by the European Union – Next Generation EU– Project "Sustainable Thermal and Acoustic self-made solutions for buildings refurbishment in disadvantaged social contexts by Reusing poor materials (STAR)" – CUP J53D23002280006 – Grant Assignment Decree No. 961 adopted on June 30, 2023 by the Italian Ministry of Ministry of University and Research (MUR).

Declaration of competing interest

The authors declare that they have no known competing financial interests or personal relationships that could have appeared to influence the work reported in this paper.

Acknowledgment

This article was written in memory of Professor Angelo Farina of the University of Parma. The authors thank Professor Farina for his contribution. JK CD is grateful to CIRCC - Consorzio Interuniversitario Reattività Chimica e Catalisi for funding.

Supplementary information

Measurements on small samples (Kundt's tube)

The Kundt's tube, or impedance tube, can be used to measure both the α and the TL. According to ISO 10534-2 (International Organization for Standardization, ISO 10534-2:2023 Acoustics - Determination of acoustic properties in impedance tubes, Part 2: Two-microphone technique for normal sound absorption coefficient and normal surface impedance, 2nd Edition 2023.), the sound absorption coefficient is measured using a set-up with two microphones and a rigid end, as shown in Fig. 5 a). The speaker emits a sine sweep with the following parameters: duration of 10 s, frequency range 50–4000 Hz (ensuring a plane wave propagation), variable amplitude between 0.05 V and 0.40 V. The signals are acquired by PCB Piezotronics 378C10 microphones connected to a data acquisition device, NI USB 4431. The distance between microphones is 30 mm according to the standard (Bengtström et al., 2016); it fixes the following limit for the distance s between microphones as $s < 0.45c/F$, where c is the sound speed, and F is the maximum considered frequency. Moreover, a distance between the sample and microphone 2 greater than 1–2 tube diameters is suggested (Katz, 2000). The acquired traces are elaborated using the Main_TL software developed by Materiacustica s.r.l. to obtain the α values.

For the measurement of the TL, the set-up is modified as illustrated in Fig. 5 b) and to comply with the so-called four-pole parameters method (Munjal, 2014). The four parameters (A, B, C, and D) relate the inlet pressure (p_i) and velocity (v_i) to respective outlet values (p_o, v_o), assuming a plane wave propagation, expressed as:

$$[p_i v_i] = [ABCD][p_o v_o] \quad \text{(S1)}$$

The impedance tube utilized in this study features a diameter of 45 mm. To calculate the four-pole parameters exploiting the transfer-matrix approach, the two-loads method (Katz, 2000) is adopted. This method requires the use of four microphones and the changing of the termination impedance. In this paper, two terminations with various lengths, terminations with and without absorbing material, and even a closed and an open-

ended termination have been implemented. For each setup configuration, three measurements were performed, moving microphone 2 to locations 3 and 4 while keeping microphone 1 in the original location. Then, defined S_i and S_o as the effective cross-sectional areas at the inlet and outlet of the test sample, the TL was calculated as:

$TL = 20\ \log f_0 10\{½|A_{23} + B_{23}/\rho c + \rho c\ C_{23} + D_{23}|\} + 10\log f_0 10(S_i/S_o)\ (S_2)$

where ρ is the fluid density, c is the speed of sound in the fluid medium, and A_{23}, B_{23}, C_{23} and D_{23} are the four-pole parameters between microphones 2 and 3 (Tao et al., 2003). To evaluate the homogeneity of the panels, three samples were tested for each panel typology, while to evaluate the repeatability of the measurements, each sample was tested three times. The curves reported in the following sections represent the average of the three repetitions for each sample, which shows a standard deviation of 0.001.

Measurements on larger samples (SONOCAT sensor)

The second set of acoustic tests was performed using a Sonocat probe. The sensor is shown in Fig. 6 a) and it is designed to measure sound characteristics in a stationary field, allowing omnidirectional capture of incident and reflected sound waves. Since it does not require sampling, it provides results that are more representative of real acoustic conditions (Saccenti et al., 2023). The sensor is equipped with a spherical array of 8 MEMS microphones (30 mm). The finite size of the probe poses limitations at very high frequencies, while the distance from the sample must be carefully controlled to optimize the measurement accuracy at low frequency. The calculation method is based on the relationship between two fundamental quantities $\alpha = \frac{W_a}{W_o}$, where W_a is the time-averaged active sound power, representing the acoustic energy actually absorbed by the sample. Both of them are calculated by integrating the respective sound intensities at the sample surface. The sound coefficient is provided with a specific value for each analyzed frequency band in thirds of an octave.

The Farina-Fausti formula, used in acoustic measurements with a PU probe (pressure–velocity probe), represents an evolution of the basic sound absorption coefficient. The PU probe combines a pressure microphone with a particle velocity sensor, allowing direct measurement of both acoustic pressure and particle velocity at the same point. This differs from traditional PP (pressure-pressure) probes, which derive velocity indirectly from the pressure gradient between two microphones, and from microphone arrays, which use multiple pressure measurements to estimate directional characteristics. The direct measurement of the velocity typically offers advantages in terms of accuracy at low frequencies and near-field measurements, while avoiding the spatial averaging inherent to PP probes and the complexity of array processing; however, it may be more sensitive to flow noise and require careful calibration.

The Farina-Fausti formula that implements this measurement approach is:

$$\alpha = \frac{4|\Re(G_{xy})|}{(G_{xx} + Gyy + 2|\Re(G_{xy})|)} \tag{S3}$$

where the term $4|R(G_{xy})|$ is proportional to the absorbed power W_{ac}, and the denominator is proportional to the incident power Win. The multiplying factor 4 is introduced to ensure normalization of the coefficient α in the range between 0 and 1. This more elaborate formulation is necessary in the context of real measurements with a PU probe, where the quantities Wac and Win must be derived through analysis of the pressure (G_{xx}) and velocity (G_{yy}) eigenspectra, as well as the pressure–velocity cross-spectrum (G_{xy}).

Data availability

Data will be made available on request.

References

Abu-Jdayil, B., Mourad, A., Hittini, W., Hassan, M., Hameedi, S., 2019. Traditional, state-of-the-art and renewable thermal building insulation materials: an overview. Constr. Build. Mater. 214, 709–735. https://doi.org/10.1016/j.conbuildmat.2019.04.102.

Al, A.H., Chawich, L., Abumousa, M., Harb, G., Abu-Jdayil, B., 2024. Heat and acoustic insulation materials for construction based on polypropylene from recycled face masks reinforced with date palm leaves. J. Build. Eng. 98, 111406. https://doi.org/10.1016/j.jobe.2024.111406.

Asdrubali, F., D'Alessandro, F., Schiavoni, S., 2015. A review of unconventional sustainable building insulation materials. Sustain. Mater. Technol. 4, 1–17. https://doi.org/10.1016/j.susmat.2015.05.002.

ASHRAE Handbook of Fundamentals, 2017 edition, chapter 26, Ashrae.

Assal, R., Michel, L., Ferrier, E., 2025. Experimental study of timber and concrete composite facade connected through bonding under thermal gradients. J. Build. Eng. 108, 112814. https://doi.org/10.1016/j.jobe.2025.112814.

Bengtström, L., Salden, M., Stec, A.A., 2016. The role of isocyanates in fire toxicity. Fire Sci Rev. 5, 1–23. https://doi.org/10.1186/s40038-016-0013-2.

Benmansour, N., Agoudjil, B., Gherabli, A., Kareche, A., Boudenne, A., 2014. Thermal and mechanical performance of natural mortar reinforced with date palm fibers for use as insulating materials in building. Energy Build. 81, 98–104. https://doi.org/10.1016/j.enbuild.2014.05.032.

Berardi, U., Iannace, G., 2015. Acoustic characterization of natural fibers for sound absorption applications. Build. Environ. 94, 840–852. https://doi.org/10.1016/j.buildenv.2015.05.029.

Commission staff working document EU guidance on energy poverty. Available at: https://energy.ec.europa.eu/publications/commission-staff-working-document-eu-guidance-energy-poverty_en. Accessed on the 18th February 2025.

N. Consten, T. Campmans, S. Bertet, Y. Wijnant, 2019. On the Measurement of Sound Power using a Cubical Arrangement of Microphones in a Small Rigid Sphere, University of Twente, DAGA 2019 - Rostock, Germany.

Dehdashti, Z., Soltani, P., Taban, E., 2024. Utilizing discarded face masks to fabricate sustainable high-performance panels for enhanced building thermal and acoustic comfort. J. Clean. Product. 446, 141304. https://doi.org/10.1016/j.jclepro.2024.141304.

Di Schio, E.R., Ballerini, V., Kašpar, J., Neri, M., Pilotelli, M., Piana, E., Valdiserri, P., 2024. Applicability of face masks as recyclable raw materials for self-made insulation panels. Energies 17, 1648. https://doi.org/10.3390/en17071648.

EAD 040005-00-1201. Factory-made thermal and/or acoustic insulation products made of vegetable or animal fibres. Available at: https://www.eota.eu/download?file=/2013/13-04-0005/ead%20for%20ojeu/ead-040005-00-1201-factory-made-thermal-acoustic-insulation-products-vegetable-animal-fibres-2015rev-2016rev_ojeu.pdf. Accessed on the.

EAD 040288-00-1201 Factory-made thermal and acoustic insulations made of polyester fibres · Notified bodies for Regulation EP and Council (EC) 305/2011. Available at: https://www.eota.eu/download?file=/2015/15-04-0288/ead%20for%20ojeu/ead%20040288-00-1201_ojeu2016.pdf. Accessed on 12th December 2025.

ECORYS - Bringing Europe's building sector into the circular economy. Available at: https://www.ecorys.com/case-studies/bringing-europes-building-sector-into-the-circular-economy/. Accessed on the 18th February 2025.

Energy poverty, EU measures to tackle energy poverty. Available at: https://energy.ec.europa.eu/topics/markets-and-consumers/energy-consumers-and-prosumers/energy-poverty_en, Accessed on the 18th February 2025.

European Organisation for Technical Assessment. What is an ETA) Available at: https://www.eota.eu/what-is-an-eta-old#:~:text=The%20European%20Technical%20Assessment%20(ETA,Short%20times%2Dto%2Dmarket. Accessed on the 23th December 2025.

Gervasini, A., 2013. Temperature Programmed Reduction/Oxidation (TPR/TPO) Methods. In: Auroux, A. (Ed.), Calorimetry and Thermal Methods in Catalysis, Springer Series in Materials Science. Springer, Berlin Heidelberg, Berlin, Heidelberg, pp. 175–195. https://doi.org/10.1007/978-3-642-11954-5_5.

Green, J., 1996. Mechanisms for flame retardancy and smoke suppression -a review. J. Fire Sci. 14 (6), 426–442. https://doi.org/10.1177/073490419601400602.

Hadded, A., Benltoufa, S., Fayala, F., Jemni, A., 2016. Thermo physical characterisation of recycled textile materials used for building insulating. J. Build. Eng. 5, 34–40. https://doi.org/10.1016/j.jobe.2015.10.007.

Halashi, K., Taban, E., Soltani, P., Amininasab, S., Samaei, E., Moghadam, D.N., Khavanin, A., 2024. Acoustic and thermal performance of luffa fiber panels for

sustainable building applications. Build., Environ. 247, 111051. https://doi.org/10.1016/j.buildenv.2023.111051.
Hassani, P., Soltani, P., Taban, E., Amininasab, S., 2024. Development and optimization of sustainable high-performance acoustic and fire retardant building panels using recycled discarded denim. J. Build. Eng. 98, 111209. https://doi.org/10.1016/j.jobe.2024.111209.
International Organization for Standardization 8301:1991 Thermal insulation - Determination of steady-state thermal resistance and related properties - Heat flow meter apparatus.
International Organization for Standardization ISO 9239-1:2010: Reaction to fire tests for floorings – Part 1: Burning behavior determination using a radiant heat source.
International Organization for Standardization ISO 1182:2020 - Reaction to fire tests for products – Non-combustibility test.
International Organization for Standardization ISO 1716:2018: Reaction to fire tests for products – Determination of gross heat of combustion (calorific value).
International Organization for Standardization ISO 11925-2:2020: Reaction to fire tests – Ignitability of products under direct flame exposure – Part 2: Single-flame source test.
International Organization for Standardization, ISO 10534-2:2023 Acoustics - Determination of acoustic properties in impedance tubes, Part 2: Two-microphone technique for normal sound absorption coefficient and normal surface impedance, 2nd Edition 2023.
Jantawee, S., Lim, H., Li, M., et al., 2023. Developing structural sandwich panels for energy-efficient wall applications using laminated oil palm wood and rubberwood-based plywood/oriented strand board. J. Wood Sci. 69, 35. https://doi.org/10.1186/s10086-023-02109-x.
Jones, A., McNicol, B., 1986. Temperature-Programmed Reduction for Solid Materials Characterization. Chemical Industries, Marcel Dekker Inc, New York, NY, USA.
Katz, B.F.G., 2000. Method to resolve microphone and sample location errors in the two-microphone duct measurement method. J. Acoust. Soc. Am. 108, 2231–2237. https://doi.org/10.1121/1.1314318.
Lee-Chiong, T.L., 1999. Smoke inhalation injury: when to suspect and how to treat. Postgrad. Med. 105, 55–62. https://doi.org/10.3810/pgm.1999.02.546.
Majumder, A., Canale, L., Mastino, C., Pacitto, A., Frattolillo, A., Dell'Isola, M., 2021. Thermal characterization of recycled materials for building insulation. Energies 14, 3564. https://doi.org/10.3390/en14123564.
Marín-Calvo, N., González-Serrud, S., James-Rivas, A., 2023. Thermal insulation material produced from recycled materials for building applications: cellulose and rice husk-based material. Front. Built Environ. 9, 1271317. https://doi.org/10.3389/fbuil.2023.1271317.
Martínez, B., Virginia Mendizabal, M., Roncero, B., Bernat-Maso, E., 2024. Lluis Gil, Towards sustainable building solutions: Development of hemp shiv-based green insulation material. Constr. Build. Mater. 414, 134987. https://doi.org/10.1016/j.conbuildmat.2024.134987.
Miraftab, M., 2018. Recycling carpet materials. In: Goswami, K.K. (Ed.), Advances in Carpet Manufacture (second Edition). the Textile Institute Book Series. Woodhead Publishing, pp. 65–77. https://doi.org/10.1016/B978-0-08-101131-7.00005-8.
Mohammadabadi, M., Yadama, V., Dolan, J.D., 2021. Evaluation of wood composite sandwich panels as a promising renewable building material. Materials 14 (8), 2083.
Munjal, M.L., 2014. Acoustics of Ducts and Mufflers, 2nd ed.;. John Wiley & Sons Ltd:, Chichester, United Kingdom. ISBN 978-1-118-44312-5.
Neri, M., Cuerva, E., Levi, E., Pujadas, P., Müller, E., Guardo, A., 2023. Thermal, acoustic, and fire performance characterization of textile face mask waste for use as low-cost building insulation material. Dev. Built Environ. 14, 100164. https://doi.org/10.1016/j.dibe.2023.100164.
O'Brien, L., Li, L., Friess, W., Snow, J., Herzog, B., O'Neill, S., 2025. Review of bio-based wood fiber insulation for building envelopes: characteristics and performance assessment. Energy Build 328, 115114. https://doi.org/10.1016/j.enbuild.2024.115114. ISSN 0378-7788.
Energy Performance of Buildings Directive. Revised energy performance of building directive. Available at https://energy.ec.europa.eu/topics/energy-efficiency/energy-efficient-buildings/energy-performance-buildings-directive_en. Accessed on the 18th February 2025.
Energy Performance of Buildings Directive. Available at https://energy.ec.europa.eu/topics/energy-efficiency/energy-efficient-buildings/energy-performance-buildings-directive_en. Accessed on the 18th February 2025.
Petkova-Slipets, R., Zlateva, P., Staneva, D., 2022. Influence of the polyester non-wovens production type on their thermal and flammability properties. J. Eng. Appl. Sci. 69, 51. https://doi.org/10.1186/s44147-022-00107-2.
Press room. Textiles and food waste reduction: New EU rules to support circular economy. Textiles and food waste reduction. Available at https://www.europarl.europa.eu/news/en/press-room/20240212IPR17625/textiles-and-food-waste-reduction-new-eu-rules-to-support-circular-economy. Accessed on the 18th February 2025.
European Commission Press-release, Circular economy for textiles: taking responsibility to reduce, reuse and recycle textile waste and boosting markets for used textiles Brussels, 5 July 2023 & Communication- EU strategy for sustainable and circular textiles & Synopsis report - Online Public Consultation on the EU Strategy for Sustainable and Circular Textiles. Available at: https://ec.europa.eu/commission/presscorner/detail/%20en/ip_23_3635. Accessed on the 18th February 2025.
Regulation (EU) No 305/2011 of the European parliament and of the council of 9 March 2011 laying down harmonised conditions for the marketing of construction products and repealing Council Directive 89/106/EEC official journal of the European Union. Accessed on the 18th February 2025.
Ribeiro, R.S., Arnela, M., Zea, E., Vila, A.P., Rodrigues, N.N.A., Giglio, T., Zara, R.B., de Melo Moura, J.D., 2025. Acoustic and thermal performance of an innovative façade constructed with Brazilian plantation wood. J. Build. Eng. 104, 112348. https://doi.org/10.1016/j.jobe.2025.112348.
Ricciardi, P., Cillari, G., Miino, M.C., 2020. Valorization of agro-industry residues in the building and environmental sector: a review. Waste Manag. Res. 38, 487–513. https://doi.org/10.1177/0734242X20904426.
Rushforth, I., Horoshenkov, K., Ting, S.N., Miraftab, M., 2007. Acoustic and mechanical properties of underlay manufactured from recycled carpet waste. Ecotextiles. 4, 15–25. https://doi.org/10.1533/9781845693039.1.15.
L. Saccenti, J. Ferrari, D. Pinardi, A. Farina, Noncontact Measurements of Sound Absorption Coefficient with a Pressure-velocity Probe, a Laser Doppler Vibrometer, and a Microphone Array. Immersive and 3D Audio: from Architecture to Automotive (I3DA), Bologna, Italy, (2023) 1-9, doi: 10.1109/I3DA57090.2023.10289528.
Sadrolodabaee, P., Hosseini, S.M.A., Claramunt, J., Ardanuy, M., Haurie, L., Lacasta, A. M., de la Fuente, A., 2022. Experimental characterization of comfort performance parameters and multi-criteria sustainability assessment of recycled textile-reinforced cement facade cladding. J. Clean. Product. 356, 131900. https://doi.org/10.1016/j.jclepro.2022.131900.
Sadrolodabaee, P., de la Fuente, A., Ardanuy, M., Claramunt, J., 2025. Limestone calcined clay cementitious (LC3) paving flags with textile waste fibers and fine recycled aggregates: Mechanical, durability and multi-criteria sustainability analysis. Const. Build. Mater. 501, 144241. https://doi.org/10.1016/j.conbuildmat.2025.144241.
Savio, L., Pennacchio, R., Patrucco, A., Manni, V., Bosia, D., 2022. Natural fibre insulation materials: use of textile and agri-food waste in a circular economy perspective. Mater Circ Econ. 6. https://doi.org/10.1007/s42824-021-00043-1.
Solis, M., Huygens, D., Tonini, D., Astrup, T.F., 2024. Management of textile waste in Europe: an environmental and a socio-economic assessment of current and future scenarios. Resour. Conserv. Recycl. 207, 107693.
Tallini, A., Cedola, L., 2018. A review of the properties of recycled and waste materials for energy refurbishment of existing buildings towards the requirements of NZEB. Energy Procedia. 148, 868–875. https://doi.org/10.1016/j.egypro.2018.08.108.
Tanguay-Rioux, F., Héroux, M., Legros, R., 2021. Physical properties of recyclable materials and implications for resource recovery. Waste Manag. 136, 195–203. https://doi.org/10.1016/j.wasman.2021.10.007.
Z. Tao, A. F. Seybert, A Review of Current Techniques for Measuring Muffler Transmission Loss, 112 (2003) 2096-2100. http://www.jstor.org/stable/44745590.
UNI EN 12667:2002 - Thermal performance of building materials and products - Determination of thermal resistance using the hot plate method with guard ring and the heat flowmeter method - Products with high and medium thermal resistance.
UNI EN 13501-1:2018 - Fire classification of construction products and building elements - Part 1: Classification using data from reaction to fire tests.
UNI EN 13823:2020: Reaction to fire tests for building products – Products excluding floorings exposed to thermal attack by a single burning item.
Renovation Wave, Achieving the renovation wave. Available at: https://energy.ec.europa.eu/topics/energy-efficiency/energy-efficient-buildings/renovation-wave_en. Accessed on the 18th February 2025.
Renovation Wave, Achieving the renovation wave. Available at: https://energy.ec.europa.eu/topics/energy-efficiency/energy-efficient-buildings/renovation-wave_en. Accessed on the 18th February 2025.
T. Yang, X. Xiong, M. Petrů, X. Tan, H. Kaneko, J. Militký, J., A. Sakuma, 2020. Theoretical and experimental studies on thermal properties of polyester nonwoven fibrous material. Materials 13, 2882.